Food & Function

ROYAL SOCIETY OF CHEMISTRY

PAPER

View Article Online
View Journal | View Issue

Cite this: *Food Funct.*, 2025, **16**, 4085

Silicon-enriched functional meat enhances colonic barrier function by regulating tight junction protein expression, oxidative stress, and inflammation responses in a diabetic dyslipidemia model†

Marina Hernández-Martín, ‡[a] Aránzazu Bocanegra, ‡[b] Alba Garcimartín,‡[b] Adrián Macho-González,‡[c] Rocío Redondo-Castillejo, ‡[b] Rosa A. García-Fernández,[d] Luis Apaza-Ticona, [d,e] Sara Bastida,‡[c] Juana Benedí, ‡[b] Francisco J. Sánchez-Muniz‡[c] and M. Elvira López-Oliva *‡[a]

Western diets are linked to metabolic disorders such as Type 2 diabetes mellitus (T2DM) and diabetic dyslipidemia, which involve hyperglycemia, insulin resistance, high plasma cholesterol levels and altered lipoprotein profiles. The T2DM progression also involves glucolipotoxicity, wherein elevated glucose and fatty acid levels induce oxidative stress and inflammation. Excessive intake of saturated fats and/or cholesterol can trigger dysbiosis, which weakens the colonic barrier, increases its permeability, and promotes chronic low-grade inflammation, thereby accelerating the progression of T2DM. Silicon, an essential trace element, has demonstrated antidiabetic, hypolipidemic, antioxidant and anti-inflammatory properties, suggesting its potential as a nutritional adjuvant in therapeutic management of T2DM and the maintenance of gut health. In this study, 24 male Wistar rats were divided into three groups: (1) an early-stage T2DM group (ED) fed a control meat incorporated into a high saturated-fat diet; (2) a late-stage T2DM group (LD) fed a control meat incorporated into a high-saturated fat and high cholesterol diet combined with streptozotocin and nicotinamide injection; and (3) a late-stage T2DM group fed a silicon enriched meat (LD-Si). Microbiota composition, lipoperoxidation and concentrations of fat, cholesterol, oxysterols and short-chain fatty acids and silicon were assayed in feces. The colonic tissue morphology, barrier integrity, antioxidant capacity and inflammatory markers were measured to evaluate the impact of silicon on colonic health and intestinal barrier function. Silicon enriched meat (Si-RM) consumption increased faecal fat and cholesterol excretion and reduced toxic luminal environments by modulating oxysterols. Si-RM consumption also enhanced colonic barrier integrity, increasing tight junction proteins and goblet cells, and exhibited antioxidant effects *via* the pNrf2 pathway and superoxide dismutase activity. Furthermore, silicon reduced the pro-inflammatory cytokines TNFα and IL-6, likely through inhibition of the TLR4/NFκB pathway. The results suggest that silicon's ability to enhance intestinal barrier integrity, reduce oxidative stress, and prevent inflammation could slow down T2DM progression, making it a promising nutritional adjuvant for managing the disease.

Received 18th December 2024,
Accepted 5th April 2025

DOI: 10.1039/d4fo06277a

rsc.li/food-function

[a]*Departmental Section of Physiology, Pharmacy School, Complutense University of Madrid, Madrid, Spain. E-mail: elopez@ucm.es; Tel: (+34) 91 394 1838*
[b]*Pharmacology, Pharmacognosy and Botany Department, Pharmacy School, Complutense University of Madrid, Madrid, Spain*
[c]*Nutrition and Food Science Department, Pharmacy School, Complutense University of Madrid, Madrid, Spain*
[d]*Animal Medicine and Surgery Department, Veterinary School, Complutense University of Madrid, 28040 Madrid, Spain*
[e]*Organic Chemistry Unit, Department of Chemistry in Pharmaceutical Sciences, Faculty of Pharmacy, Complutense University of Madrid, Spain*

† Electronic supplementary information (ESI) available. See DOI: https://doi.org/10.1039/d4fo06277a

‡ AFUSAN Group, Sanitary Research Institute of the San Carlos Clinical Hospital (IdISSC), Spain.

1. Introduction

Oxidative stress induced by nutritional overload, such as Western diets rich in saturated fats and cholesterol, has traditionally been associated with the development of metabolic disorders such as type 2 diabetes mellitus (T2DM) and dyslipidemia.[1] Diabetic dyslipidaemia is characterized by hyperglycemia and insulin resistance (IR), as well as high plasma cholesterol levels and an altered lipid profile, all of which induce further exacerbation of oxidative stress.[2] This leads to a condition known as glucolipotoxicity. In this state, the concurrent exposure to high levels of glucose and free fatty acids and cholesterol exerts synergistic toxic effects, increasing free-radical activity and lipid peroxidation, which in turn contribute to the development of diabetic complications.[3] In late-stage T2DM, persistent glycolipotoxicity triggers β-cell dysfunction, apoptosis,[4] and inflammation[5] mediated by a nuclear factor kappa-light-chain-enhancer of activated B cells (NFkβ), further exacerbating insulin deficiency.[6]

The loss of barrier integrity is closely linked to the onset of metabolic disorders, including T2DM.[7] The gastrointestinal mucosa is continuously exposed to a harsh environment and toxins, leading to mucosal damage. *In vitro* exposure to the intestinal content isolated from prediabetic mice fed a high-fat diet (HFD) directly disrupted tight junction (TJ) proteins, increasing intestinal permeability.[8,9]

Factors contributing to this disruption include the gut microbiota[10] and their secreted products and toxins (such as lipopolysaccharide (LPS) and digestive enzymes, short-chain fatty acids (SCFA), and bile acids).[11] Oxysterols, oxidized cholesterol metabolites, serve as biomarkers of oxidative stress and play a role in glucolipotoxicity, leading to T2DM and dyslipidemia.[12–14] The loss of intestinal barrier integrity and the subsequent translocation of bacteria or bacterial products, such as endotoxins, from the intestine to other tissues are now considered key drivers of chronic low-grade inflammation in T2DM.[15] LPS-mediated TLR4 activation triggers systemic inflammation, contributing to IR and metabolic dysfunction.[16] Persistent low-grade inflammation accelerates metabolic disease progression, increasing oxidative stress, dysbiosis, and altered permeability.[17,18] These findings introduce a novel perspective on T2DM pathophysiology, highlighting the potential of nutritional and pharmacological interventions to regulate intestinal barrier function.[19] Meat consumption, especially processed and red meat, is a risk factor for T2DM due to its high fat and cholesterol content, as well as the presence of heme iron and arginine.[20] Consequently, meat consumption is not recommended for patients with T2DM.[21] However, since meat is widely consumed, enhancing its nutritional profile through bioactive ingredients could be a viable strategy for metabolic disease management. In this context, silicon, an essential trace element, available in the diet in drinking water and certain cereals, has gained attention for its metabolic benefits. It plays a key role in bone mineralization, connective tissue integrity, and collagen synthesis. Research suggests that it may help reduce the risk of atherosclerosis by mitigating dyslipidemia, modulating lipid metabolism, and supporting endothelial function. Silicon contributes to vascular health, antioxidant defence, and metabolic stability, highlighting its potential protective effects against cardiovascular and degenerative diseases.[22] We have previously demonstrated that the consumption of a silicon-enriched functional meat (Si-RM) exerts hypoglycemic and hypolipidemic effects, improving lipoprotein profiles by reducing cholesterol absorption and increasing its efflux in the proximal small intestine.[23–25] Additionally, Si-RM has antioxidant and anti-inflammatory properties, enhancing enzymatic antioxidant activity and suppressing proinflammatory cytokines.[26] Based on these effects, this study aims to investigate the potential of Si-RM consumption as a functional food and its feasibility as a dietary intervention aimed at enhancing intestinal health, modulating systemic inflammation, and improving metabolic homeostasis in a diabetic dyslipidemic rat model. Specifically, we evaluated its effects on: 1) oxysterol excretion and fecal lipid peroxidation, (2) gut microbiota diversity and SCFA production, (3) intestinal barrier integrity, (4) redox balance, antioxidant defences, and proinflammatory markers, and (5) histopathological markers of colonic health.

2. Materials and methods

2.1. Diets

The formulation and composition of the diets are detailed in ESI Table S1.† The control meat matrix (RM) was prepared using a 50 : 50 blend of lean minced pork and beef with lard, processed using a grinder–homogenizer (Stephan Universal Machine UM5, Stephan u. Söhne GmbH, Germany), freeze-dried, and ground into a homogeneous powder. Silicon-enriched meat (Si-RM) was prepared similarly, incorporating organic silicon (Silicium organique G57™; Glycan Group, Geneva, Switzerland) to achieve a final silicon concentration of 20 mg kg^{-1} diet.[25]

2.2. Animal model and experimental design

Twenty-four two-month-old male Wistar rats (Harlan S.L., Barcelona, Spain) were housed at the Animal Experimentation Center of Alcalá University, Madrid, Spain (registration number: ES280050001165), and grouped in pairs under controlled temperature (22.3 ± 1.9 °C) and light (12 h light/dark cycle) conditions. The study was approved by Spanish regulatory authorities (AGL2014-53207-C2-2-R) and adhered to Directive 2010/63/EU and ARRIVE guidelines.

Following previous models,[27–30] a late-stage T2DM (LD) rat model with dyslipidemia, hyperglycemia, and reduced insulin production was used, alongside an early-stage T2DM (ED) model as a reference. To induce the ED model, eight rats were fed a RM based high-saturated-fat diet (HSFD) for eight weeks. The remaining 16 rats were fed a high-saturated-fat, high-cholesterol diet (HSFHCD) for three weeks. At the fourth week, they also received an intraperitoneal injection of streptozotocin (STZ, 65 mg per kg b.w.) and nicotinamide (NAD, 225 mg per

kg b.w.) (both from Sigma-Aldrich, Madrid, Spain). Four days later, once fasting hyperglycaemia was confirmed, the HSFHCD fed animals were divided into two groups: the late-stage T2DM control (LD) group that continued RM and HSFHCD for another five weeks and the LD group supplemented with 2 mg kg^{-1} Si-RM (LD-Si) until the end of the experiment. The silicon dosage was selected based on Western *vs.* Eastern population consumption patterns.[31] Details of the diet are provided in Table S1.†

At the end of the experiment, the rats were anesthetized with isoflurane (5% v/v), and blood was collected from the descending aorta. The distal colon was dissected, measured, weighed, and processed for further analyses.

2.3. Faecal analysis: weight, moisture, lipids, cholesterol, lipid peroxidation (TBARS), and silicon content

Faeces were collected daily during the final week of the experiment, weighed, and frozen at −20 °C until analysis. The moisture content in faeces was determined by oven drying at 100 °C to a constant weight.[32]

Faecal fat was extracted following the method reported by David *et al.*[33] Briefly, 1 g of dried faeces was hydrated, homogenized, extracted using a chloroform/methanol (1 : 1) mixture, centrifuged at 750*g* for 10 min, and the organic phase was collected. Solvent evaporation was performed using a rotary evaporator (Rotavapor R-200, Büchi, Barcelona, Spain). Cholesterol quantification was performed after extraction from 0.25 g of dried faeces, with resuspension in isopropanol (95 : 5) and analysis using 15 μL of the sample + 150 μL of working reagent.

The silicon content of the faecal samples was measured after acid digestion (HNO_3, H_2O_2, and HF) using inductively coupled plasma optical emission spectrometry (ICP-OES) at ICTAN-CSIC. International reference materials were used for accuracy.

For lipid peroxidation quantification (TBARS assay), faecal samples (150 mg) were extracted in 1 mL water at 37 °C for 1 h, centrifuged, and analyzed using 200 μL faecal water + 40 μL SDS (20%) + 600 μL sodium acetate buffer (pH 4) + 600 μL TBA (0.8%, pH 4). Data were expressed as μg MDA per g faeces.

2.4. Determination of oxysterols in faeces

Faecal oxysterols were analyzed using solid–liquid microextraction (SLME) and nuclear magnetic resonance (NMR) spectroscopy. All solvents were of analytical grade and used without further purification. Reference standards included 24(*S*)-hydroxycholesterol (24-OHC), 25-hydroxycholesterol (25-OHC), 27-hydroxycholesterol (27-OHC), cholesterol 5α,6α-epoxide (5,6-EC), 7β-hydroxycholesterol (7-OH), and 7α-hydroperoxycholesterol (7-OOH) (Sigma-Aldrich, Madrid, Spain). Faecal samples (50–60 mg) were extracted with chloroform (50 mL, 3×), concentrated to 1 mg, and resuspended in 160 μL $CDCl_3$-d_1 before transfer to NMR microtubes. NMR spectra were acquired on a Bruker Avance AV (5 mm Dual 1H-13C probe, 300 MHz) with 256 transients, 128 K points, a spectral width of 14 ppm, an acquisition time of 4.0 s, and a delay time of 2.0 s per sample, following a modified spin echo sequence with a double pulse field gradient.[34] Spectral data were processed using MestReNova software (v14.1.2, MestReC, Spain), applying Fourier transformation with 0.3 Hz line broadening, manual phase, and baseline corrections. Chemical shifts (δ) were referenced to $CDCl_3$-d_1 (7.26 ppm), and peak patterns were identified using standard notations: s (singlet), d (doublet), t (triplet), q (quartet), quint (quintet), sext (sextuplet), sept (septuplet), m (multiplet), and br (broad signal).

2.5. Histological procedure and immunohistochemical staining

Distal colonic samples were fixed in 10% formaldehyde, embedded in paraffin, and cut into 3 μm-thick sections. The sections were stained with hematoxylin–eosin (H&E), periodic acid Schiff (PAS), and Alcian Blue (AB, pH 2.5) for histological analysis. Images were captured with a Leica DM LB2 light microscope and a Leica DFC 320 camera (Leica, Madrid, Spain), and analysed with ImageJ software (Fiji image J; 1.54j, NIH, USA). Crypt depth was measured from the H&E sections by counting the number of cells per hemi-crypt, focusing only on crypts with an open longitudinal axis. The level of neutral mucin glycoprotein in the tissue was assessed by PAS and AB staining and calculated as the number of PAS or AB-positive cells per crypt. For immunohistochemistry, the sections were deparaffinized, rehydrated, and subjected to antigen retrieval in 10 mM citrate buffer (pH 6.0). After blocking with 3% hydrogen peroxide, the sections were incubated overnight at 4 °C with the appropriate biotinylated secondary antibody. Staining was performed using a streptavidin-biotin horseradish peroxidase (HRP) system and developed with 3,3′-diaminobenzidine (DAB) (Sigma-Aldrich, Madrid, Spain). Counterstaining was performed with Harris's hematoxylin. Brown colour indicates specific protein immunostaining and light blue colour indicates nuclear haematoxylin staining. Positive and negative controls were used during the optimization of the methods. Immunoreactivity was quantified based on the immunoreactivity score (IRS), categorized as weak (1), moderate (2), diffuse (3), or intense (4). A total of 10 fields per section per rat were analyzed by two blinded researchers.

2.6. Assessment of apoptosis: terminal deoxynucleotidyl transferase dUTP nick end labeling (TUNEL) procedure

Colonic sections were deparaffinized, rehydrated, and permeabilized with proteinase K (20 μg mL^{-1}) for 15 min at 37 °C. Endogenous peroxidase activity was quenched with 3% hydrogen peroxide for 10 min, after which they were washed with PBS. The sections were then incubated with equilibration buffer for 10 min, after which the terminal deoxynucleotidyl transferase reaction mixture was applied to all sections except the negative control and incubated at 37 °C for 1 h. The reaction was stopped by placing the sections in saline-sodium citrate buffer for 15 min. Incorporated biotinylated nucleotides were detected using streptavidin-HRP (1 : 500) for 30 min at

room temperature. After multiple washes, the sections were treated with DAB until a colour developed (5–10 min). Finally, the sections were dehydrated, mounted, and stained with Harris' hematoxylin. The number of apoptotic positive nuclei per crypt was then counted.

2.7. Analysis of antioxidant (SOD, CAT, GR and GPx) activities and oxygen radical absorbance capacity (ORAC)

Superoxide dismutase (SOD) activity was measured *via* a modified nitroblue tetrazolium (NBT) assay.[35] The absorbance of the nitrite-EDTA complex was recorded at 560 nm every minute for 10 min at 37 °C using a SPECTROstar Nano spectrophotometer (BMG LABTECH, Germany).

Catalase (CAT) activity was determined by monitoring H_2O_2 degradation at 260 nm every 30 s for 10 min.[36]

Glutathione reductase (GR) activity was measured *via* NADPH oxidation to $NADP^+$ during GSSG reduction, recording the absorbance decrease at 340 nm.[37]

Glutathione peroxidase (GPx) activity was quantified by NADPH oxidation in the presence of cumene hydroperoxide, recording 340 nm absorbance every minute for 10 min.[38]

Protein normalization for all enzyme activities was standardized to protein concentration[39] (SPECTROstar Nano) and expressed as nmol min^{-1} mg^{-1} protein.

The oxygen radical absorbance capacity (ORAC) assay was performed on colonic mucosal extracts following Ou *et al.* (2001).[40] Fluorescence intensity was recorded every minute for 2 h using a FLUOstar Omega plate reader (BMG LABTECH, Germany) at 485 nm (excitation) and 535 nm (emission). Data were expressed as μmol Trolox equivalents (TE) g^{-1} colonic mucosa.

2.8. Reduced (GSH) and oxidized (GSSG) glutathione

GSH and GSSG levels were measured using the method by Senft *et al.* (2000)[41] with *ortho*-phthalaldehyde (OPA) as a fluorescent probe. Distal colonic mucosal extracts were deproteinized with redox quenching buffer (5% TCA-RQB), homogenized by sonication at 4 °C, and centrifuged (14 000*g*, 10 min). For GSH determination, the samples were mixed with RQB, 3.15 mM *N*-ethylmaleimide, 0.1 M phosphate buffer, and OPA (5 mg mL^{-1} in methanol). GSSG quantification involved reducing GSSG to GSH using 95.62 mM dithionite, followed by the same detection protocol. Fluorescence was measured at an excitation wavelength of 360 nm and an emission wavelength of 460 nm using a FLUOstar Omega plate reader (BMG LABTECH, Germany). The results were expressed as nmol mg^{-1} protein, and the GSH/GSSG ratio was calculated.

2.9. DNA extraction and 16S rRNA gene sequencing

Faecal samples were collected from the distal colon and immediately stored in sterile tubes at −80 °C. They were subsequently analyzed as described by Macho-González *et al.* (2021).[42] Bacterial DNA was extracted from 180–220 mg of each faecal sample using an optimized protocol, which included homogenization with glass beads on the FastPrep system (MP Biomedicals, California, USA) followed by DNA extraction with the QIAamp DNA Stool Mini Kit (Qiagen NV, Venlo, Netherlands), according to the manufacturer's instructions. The extracted DNA was stored at −80 °C until its concentration was measured using a NanoDrop spectrophotometer ND-1000 (Thermo Fisher Scientific, Wilmington, USA).

To assess faecal bacterial diversity, the V3–V4 hypervariable regions of the bacterial 16S rRNA genes were amplified using the universal primers 343 F (5′-TACGGRAGGCAGCAG-3′) and 798 R (5′-AGGGTATCTAATCCT-3′). Real-time PCR (qPCR) was then performed to detect 16S rDNA using bacterial group-specific primers. The qPCR experiments were carried out on the AriaMix system (Agilent Technologies, Palo Alto, CA, USA) using SYBR Green qPCR Master Mix (Agilent Technologies, Palo Alto, CA, USA), following the amplification protocols outlined by Redondo-Castillejo *et al.* (2023).[70] A standard curve was used in each qPCR assay for quantification of target bacterial DNA.

2.10. Faecal SCFA determination

SCFA levels were measured following Álvarez-Cilleros *et al.*[43] Under sterile conditions, 0.1 g of faecal matter was mixed with 1 mL of water + 0.5% phosphoric acid and stored at −20 °C. The samples were homogenized (2 min, vortex), centrifuged (17 949*g*, 10 min), and analyzed using a gas chromatograph-mass spectrometer (GC-MS, Agilent 7890A, Agilent Technologies, Spain) equipped with a DB-WAX column (60 m, 0.25 mm, 0.25 μm, Agilent). The ionization source and quadrupole temperatures were set at 230 °C and 150 °C, respectively. Detection was performed in single ion monitoring mode, and a calibration curve (2–10 000 μM) was generated using WSFA-2 (Sigma-Aldrich, Spain) and 4-methylvaleric acid (Sigma-Aldrich, Spain) as an internal standard. SCFA concentrations were expressed as μmol g^{-1} faeces and as percentages.

2.11. Colonic marker concurrence/scores

Average colonic marker scores were calculated according to the method outlined by Macho-González *et al.*[42] The mean score was determined by assigning values 1, 2, or 3 to the 1st, 2nd, and 3rd tertiles, respectively, and taking into account the number of rats in each tertile. A score of 3 was assigned to the highest-value measurements and 1 to the lowest ones, except for the anti-inflammatory score of the A&A index, where higher values of inflammation markers place them in a lower tertile. The gut microbiota (GM index) was derived by considering four genera and species: *Bifidobacterium* spp., *Faecalibacterium prausnitzii*, *Lactobacillus* spp., and Enterobacteriaceae, with the index value calculated by summing the tertile values for each parameter. The total SCFA index was calculated by considering both branched-chain and straight-chain fatty acids. The colon morphology index (CM index) incorporated parameters such as crypt depth, crypt density, the number of positive goblet cells per crypt, the PCNA index, and the TUNEL index. The TJ index was obtained by summing the tertile values for occludin and ZO-1. The antioxidant and anti-inflammatory index (A&A index) were the sum of the following parameters: Mn-SOD, Cu/Zn-SOD, catalase, GPx, GR, HO1, 40 serine phospho-nuclear

erythroid 2-related factor 2 (pNrf2), GSH/GSSG ratio, nitrotyrosine, TNFα, IL-6, pNFκB p65, and TLR4. Finally, the global colonic index (GC index), representing a composite marker of 17 variables, was calculated by summing the tertile values for the GM index, SCFA index, CM index, TJ index, and A&A index.

2.12. Statistical analysis

All data are presented as mean ± standard deviation (SD). Multiple group comparisons were performed using one-way ANOVA, followed by the Bonferroni *post-hoc* test for homogeneous variances or the Tamhane test for heterogeneous variances. Non-parametric variables were analyzed using the Kruskal–Wallis test, followed by the Dunn–Bonferroni *post-hoc* test. Pearson's correlation was used for continuous variables, while Spearman's correlation was applied to score-based indices. Statistical significance was set at $p < 0.05$. Statistical analyses were conducted using SPSS v25.0 (SPSS Inc., Chicago, IL, USA) and GraphPad Prism v8.1.2 (GraphPad Software, La Jolla, CA, USA).

3. Results

3.1. Effect of silicon on biochemical parameters in plasma

Table S3† presents data on plasma glucose, insulin levels, the HOMA-β index, triglycerides, cholesterol, atherogenic index (AI), diabetes trend score (DTscore), and dyslipidemic diabetes score (DDscore). The results revealed significant differences in plasma, insulin, HOMA-β ($p < 0.001$), and DTscore ($p < 0.001$) among the experimental groups. Rats in the LD group exhibited significantly higher plasma glucose levels ($p < 0.001$), but lower insulin levels and HOMA-β ($p < 0.001$) compared to the ED group. The LD-Si rats displayed intermediate values, with significant differences observed in all parameters ($p < 0.01$) compared to both the LD and ED groups. Notably, all groups had high plasma glucose levels (≥11.1 mmol L^{-1}), indicating severe hyperglycemia.

The treatment also had a significant effect on plasma triglycerides, cholesterol, and the AI, calculated as total cholesterol/HDL cholesterol (ANOVA $p < 0.01$). The prevalence of high triglycerides (≥1.69 mmol L^{-1}) and high cholesterol (≥2.59 mmol L^{-1}) differed significantly across the experimental groups (Chi-square test $p < 0.001$). Hypertriglyceridemia was observed in 62.5% of the ED rats but was absent in both the LD and LD-Si groups. Conversely, hypercholesterolemia was prevalent in 87.5% of the LD rats but was not observed in the ED and LD-Si groups. The LD group had significantly higher cholesterol levels and AI compared to the ED group ($p < 0.001$). However, the elevated cholesterol levels in the LD group were reversed by silicon treatment, bringing them in line with those of the ED group. The LD and LD-Si rats exhibited lower triglycerides and higher AI ($p < 0.01$) compared to the ED rats.

Both the DTscore and DDscore showed significant differences among the experimental groups (ANOVA $p < 0.001$). The LD rats had significantly higher DTscore and DDscore compared to the ED and LD-Si rats ($p < 0.001$). The LD-Si group exhibited significantly lower DTscores compared to LD (28.3%, $p < 0.001$) groups. Additionally, the LD-Si group had a lower DDscore compared to the LD group, with no significant differences observed between the ED and LD-Si groups ($p < 0.05$). These findings suggest that silicon (Si-RM) improved the plasma diabetic dyslipidemia parameters in rats with late-stage T2DM.

3.2. Effects of silicon on colonic length and weight, faecal weight and moisture, content of fat, cholesterol and silicon in faeces, faecal lipoperoxidation and oxysterol content

Table 1 presents data on the length and weight of the colon, stool moisture, fat, cholesterol, and silicon contents, as well as

Table 1 Colon length and weight, faecal parameters and lipoperoxidation and oxysterol content of early-stage diabetes (ED), late-stage diabetes (LD), and late-stage diabetes-silicon (LD-Si) groups

	ED group	LD group	LD-Si group	*p*
Colon length (cm)	14.88 ± 1.36	15.31 ± 1.91	16.43 ± 1.64	NS
Empty colon weight (g)	1.94 ± 0.45^{b}	1.41 ± 0.32^{a}	1.69 ± 0.26^{a}	0.025
Faeces weight (g per d dry matter)	1.14 ± 0.08^{a}	1.59 ± 0.06^{b}	1.96 ± 0.24^{c}	<0.001
Faeces moisture (g day^{-1})	0.19 ± 0.03^{a}	0.27 ± 0.04^{b}	0.32 ± 0.05^{b}	<0.001
Faeces fat excretion (mg g^{-1})	80.01 ± 6.6^{a}	170.61 ± 10.1^{b}	254.02 ± 14.2^{c}	<0.001
Faecal cholesterol excretion (mg g^{-1} day^{-1} dry matter)	1.72 ± 0.51^{a}	21.25 ± 1.26^{b}	48.31 ± 10.77^{c}	<0.001
Faecal silicon excretion (μg g^{-1} day^{-1} dry matter)	2.95 ± 0.86^{a}	2.73 ± 0.84^{a}	6.42 ± 2.04^{b}	<0.001
TBARS (μg MDA g^{-1} faeces)	59.71 ± 3.34^{a}	66.4 ± 2.97^{b}	60.96 ± 6.91^{ab}	<0.05
RMN oxysterols (ppm)				
24-OHC	30.06 ± 3.21^{c}	1.51 ± 0.11^{a}	14.97 ± 0.75^{b}	<0.001
25-OHC	0.57 ± 0.02^{a}	2.12 ± 0.01^{b}	0.66 ± 0.002^{a}	<0.001
27-OHC	8.47 ± 0.02^{a}	31.53 ± 0.02^{b}	9.73 ± 0.007^{a}	<0.001
5,6-EC	0.14 ± 0.01^{b}	0.075 ± 0.001^{a}	0.097 ± 0.001^{a}	<0.001
7-OH	0.072 ± 0.002^{a}	0.13 ± 0.001^{c}	0.11 ± 0.001^{b}	<0.001
7-OOH	0.12 ± 0.001^{b}	0.14 ± 0.003^{c}	0.10 ± 0.001^{a}	<0.001

Values expressed as mean ± SD ($n = 8$ per group). Labeled means in a row bearing different letters ($a < b < c$) were significantly different (at least $p < 0.05$ with ANOVA followed by Scheffe or Tamhane *post-hoc* test). NS: no significant differences between groups. 24-OHC, 24-hydroxycholesterol; 25-OHC, 25-hydroxycholesterol; 27-OHC, 27-hydroxycholesterol; 5,6-EC, 5,6-epoxicholesterol; 7-OH, 7-hydroxycholesterol; and 7-OOH, 7-hydroperoxycholesterol.

faecal lipid peroxidation. Additionally, Table 1 also displays the faecal concentrations of 24-hydroxycholesterol (24-OHC), 25-hydroxycholesterol (25-OHC), 27-hydroxycholesterol (27-OHC), 5,6-epoxycholesterol (5,6-EC), 7-hydroxycholesterol (7-OH), and 7-hydroperoxycholesterol (7-OOH). Fig. 1 shows ^{1}H NMR spectra of oxysterols.

No differences were found in colon lengths between groups; however, the weight of the empty colon was lower in the LD rats compared to that of the ED rats. Although silicon slightly increased the colon weight, it did not reach the levels observed in the ED group ($p = 0.025$).

LD rats showed higher faecal weight ($p < 0.0001$), moisture ($p < 0.001$), fat ($p < 0.0001$), and cholesterol ($p < 0.0001$) compared to ED rats. Daily silicon excretion showed no significant differences between these two groups. In contrast, LD-Si rats exhibited significantly higher values for all parameters, except for faecal moisture, which also tended to increase. It is important to highlight that fat and cholesterol excretion in the faeces in the LD-Si group was significantly higher, being 2.1 and 28.1 times higher than that in the ED group and 1.5 and 2.3 times ($p < 0.001$) higher than that in the LD group, respectively.

Regarding lipid peroxidation measured with the TBARS technique, LD rats showed significantly higher values than those in the ED group ($p < 0.001$). The LD-Si group did not display significant differences with the other study groups.

Upon analysing all the ^{1}H NMR spectra of oxysterols (Fig. 1), the predominant presence of hydroxylated cholesterol derivatives was observed, with variations depending on the treatment group. In the ^{1}H NMR spectrum of the ED group, intense signals were detected at 2.82 (d, J = 13.7 Hz, 1H-24) ppm, corresponding to the side chain of 24-OHC. Additionally, low-intensity signals were observed at 2.38–2.27 ppm (m, 1H-4), corresponding to 5,6-EC. In the ^{1}H NMR spectrum of the LD group (Fig. 1), intense signals were found at 1.24–1.17 ppm (m, 2H-24,24′), corresponding to the side chains of 25-OHC and 27-OHC. Low-intensity signals were also detected at 2.19 ppm (d, J = 11.4 Hz, 1H-4), corresponding to 7-OH. Finally, in the ^{1}H NMR spectrum of the LD-Si group (Fig. 1), intense signals were detected at 0.93–0.81 ppm (m, H-25), corresponding to the side chains of 27-OHC and 24OHC. Low-intensity signals at 2.96 (d, J = 44.4 Hz, 2H-7,8) ppm, corresponding to 7-OOHC, were also identified.

As shown in Table 1, LD rats exhibited significantly lower levels of 24-OHC and 5,6-EC ($p < 0.0001$), but higher levels of 25-OHC and 27-OHC compared to the ED rats ($p < 0.0001$). In contrast, the LD-Si group demonstrated lower levels of 24-OHC and 5,6-EC compared to the ED group, but these were higher than those observed in the LD group, with 24-OHC levels increasing by 891.35% ($p < 0.0001$) and that of 5,6-EC by 62.60% ($p < 0.0001$). The levels of 25-OHC, 27-OHC, and 7-OH were significantly higher in the LD-Si group than in the ED group, although still lower than those in the LD group ($p < 0.0001$). For 7-OOH, the LD group exhibited a significant increase in its levels compared to the ED group, whereas the LD-Si group showed a significant decrease in 7-OOH levels compared to the ED group.

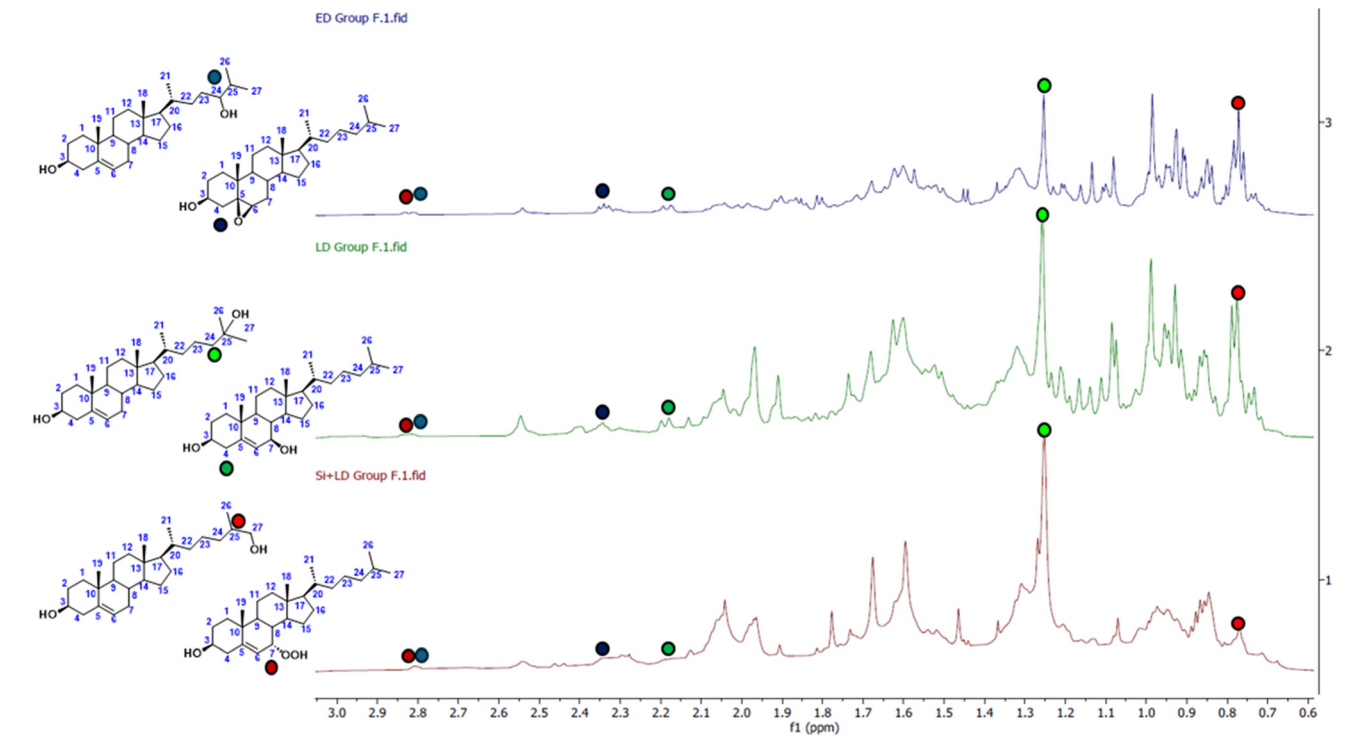

Fig. 1 Identification of oxysterols in the ^{1}H NMR spectrum from early-stage diabetes (ED), late-stage diabetes (LD), and late-stage diabetes-silicon (LD-Si) groups.

3.3. Silicon effects on the gut microbiota

Table 2 presents the bacterial groups of the gut microbiota in the study, classified by gender (ANOVA, $p < 0.05$). The three groups showed no significant differences in the abundance of microbiota species such as *Enterobacteriaceae* spp., *Bacteroides* spp., *Lactobacillus*, *B. coccoides*, *C. leptum*, *Bifidobacterium* spp., and *Enterococcus* in the faecal samples analysed. The only exception was observed in *F. prausnitzii*, which showed a significant decrease in colonic levels in the LD group (8.22%) compared to the ED group ($p < 0.001$). The addition of silicon resulted in a slight increase in *F. prausnitzii* levels (8.44%), but this change was not statistically significant when compared to the LD group.

3.4. Effect of silicon on short chain fatty acid levels in colonic faeces

The SCFA levels extracted from the colonic faecal material are presented in Table 3 (ANOVA, $p < 0.05$).

No significant differences were observed in the concentrations of propionic acid, isobutyric acid, valeric acid, and isovaleric acid across the groups. The ED group showed the lowest and highest levels of acetic acid, being significantly different from both LD and LD-Si groups, and lying between them ($p < 0.05$). Moreover, ED had the highest concentration of butyric acid showing significant differences from LD and LD-Si ($p < 0.001$) which, as previously mentioned, did not differ significantly between them.

3.5. Effect of silicon on morphological parameters and barrier integrity of the distal colon

Fig. 2 displays mucosal morphological parameters such as crypt density (Fig. 2B) and crypt depth (Fig. 2C), number of stained PAS and AB positive cells (Fig. 2D), and levels of occludin and ZO-1(Fig. 2E). Fig. 2A shows representative photographs of these parameters from slices of colonic distal mucosa.

The results showed that LD rats exhibited a significant decrease in crypt density, goblet cell number/crypt, and levels of occludin and ZO-1 ($p < 0.001$) in comparison with ED ones, while there were no significant differences in colonic crypt depth ($p > 0.05$).

Silicon improved the morphology and integrity of the colonic barrier. The LD-Si group displayed a significant increase in crypt depth ($p < 0.001$) with respect to both ED and LD groups, while the crypt density was lower than that of the ED group and higher than that of the LD group (both $p < 0.01$). The number of goblet cells per crypt was significantly higher in LD-Si rats compared to those in ED (PAS:36.13%; AB:22.5%, $p < 0.001$) and LD (PAS:74.36%, AB: 164.3%, $p < 0.0001$) rats. Occludin and ZO-1 levels were higher in LD-Si rats compared to those in LD rats ($p < 0.001$), achieving values of ED rats ($p > 0.05$).

3.6. Effect of silicon on proliferation and apoptosis balance in the epithelium of distal colonic mucosa

Fig. 3 shows photographs (Fig. 3A) and IRS of PCNA-LI (Fig. 3B), TUNEL-LI (Fig. 3C) and caspase 3 levels (Fig. 3D) from colonic mucosa slices.

Regarding proliferation, LD rats showed significantly higher levels than ED ones ($p < 0.001$) in all parameters, increasing the epithelial turnover in the colonic mucosa. Silicon decreased the PCNA-LI levels compared to those in the LD group, with no significant difference between LD-Si and ED groups ($p > 0.05$). Although there was a tendency to decrease

Table 3 Faecal short chain fatty acid levels of early-stage diabetes (ED), late-stage diabetes (LD) and late-stage diabetes-silicon (LD-Si) groups in μmol g^{-1} faeces

	ED group	LD group	LD-Si group	*p*
Acetic acid	30.84 ± 5.45^{c}	24.04 ± 3.76^{b}	20.77 ± 5.72^{a}	<0.01
Propionic acid	6.87 ± 1.30	7.86 ± 3.58	6.57 ± 2.53	NS
Butyric acid	7.90 ± 2.38^{b}	1.18 ± 0.32^{a}	1.72 ± 0.43^{a}	<0.001
Isobutyric acid	0.60 ± 0.16	0.51 ± 0.16	0.42 ± 0.08	NS
Valeric acid	0.69 ± 0.21	0.59 ± 0.29	0.40 ± 0.12	NS
Isovaleric acid	0.68 ± 0.35	0.49 ± 0.14	0.34 ± 0.11	NS

Values expressed as mean (μmol g^{-1} faeces) ± SD ($n = 7$ per group). Labelled means in a row bearing different letters ($a < b < c$) were significantly different (at least $p < 0.05$ ANOVA followed by Scheffe or Tamhane *post-hoc* test). NS: o significant differences between groups.

Table 2 Main bacterial groups quantified by PCR in faeces of early-stage diabetes (ED), late-stage diabetes (LD) and late-stage diabetes-silicon (LD-Si) groups

	ED group	LD group	LD-Si group	*p*
Enterobacteriaceae spp.	6.84 ± 0.32	7.16 ± 0.80	6.70 ± 0.57	NS
Bacteroides spp.	9.66 ± 0.35	9.24 ± 0.35	9.43 ± 0.51	NS
Lactobacillus spp.	8.70 ± 0.46	8.24 ± 0.29	8.26 ± 0.78	NS
C. Coccoides	11.89 ± 0.39	11.98 ± 0.24	11.74 ± 0.35	NS
C. leptum	8.34 ± 0.42	8.24 ± 0.13	7.84 ± 0.54	NS
Bifidobacterium spp.	7.01 ± 0.89	6.25 ± 0.33	6.38 ± 0.47	NS
Enterococcus spp.	6.14 ± 0.49	6.36 ± 0.72	5.94 ± 0.34	NS
F. Prausnitzii	9.01 ± 0.41^{a}	8.22 ± 0.32^{b}	8.44 ± 0.20^{b}	<0.001

Values expressed as mean (Lg CFU g^{-1} faeces) ± SD ($n = 8$ per group). Labelled means in a row bearing different letters ($a < b <$ c) were significantly different (at least $p < 0.05$ ANOVA followed by Scheffe or Tamhane *post-hoc* test). NS: no significant differences between groups and CFU: colony-forming units.

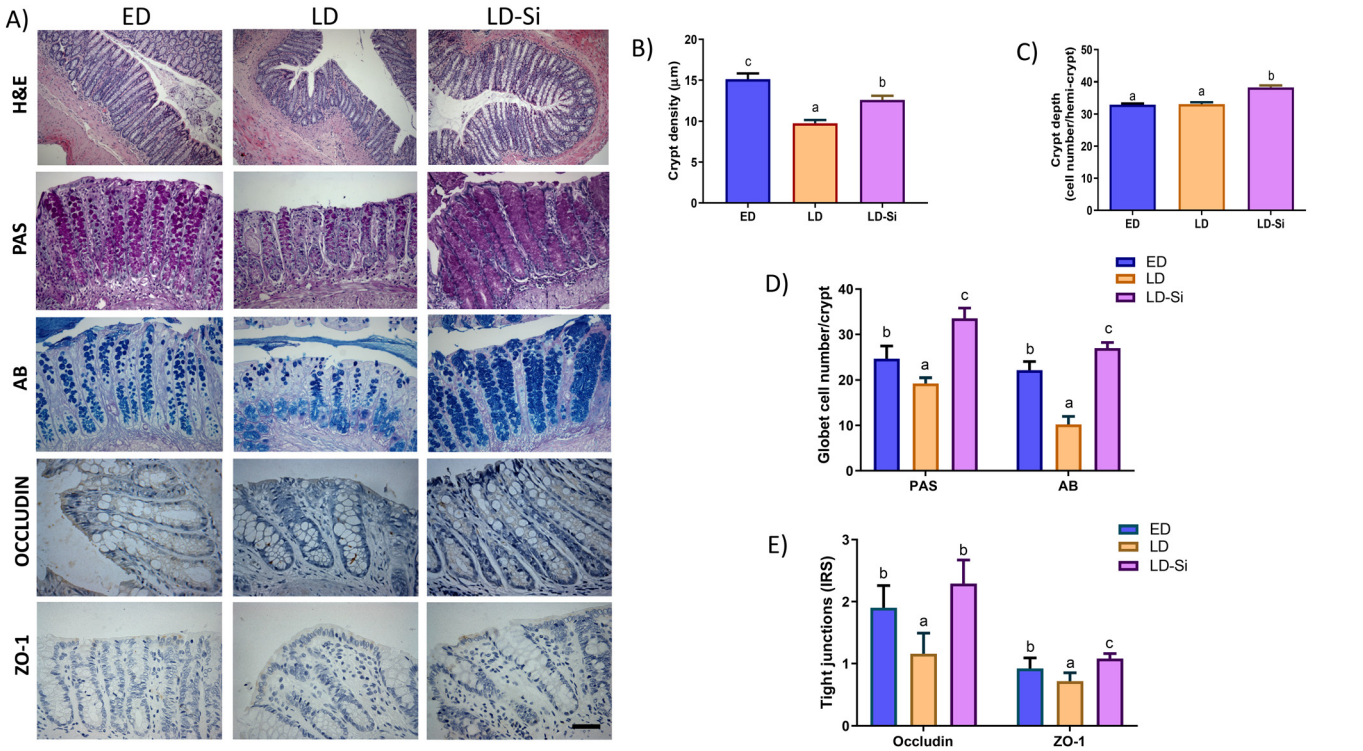

Fig. 2 Colonic morphometric markers in early-stage diabetes (ED), late-stage diabetes (LD), and late-stage diabetes-silicon (LD-Si) groups. (A) Representative images of H&E, PAS, and AB staining, and immunohistochemical labeling of occludin and ZO-1 antibodies, scale-bar: 50 µm, (B) crypt density (µm), (C) crypt depth (cell number/hemi-crypt), (D) PAS and AB (goblet cell number per crypt), and (E) immunoreactivity scores of occludin and ZO-1. Values expressed as mean ± SD. Different letters ($a < b < c$) indicate significant differences between groups, ANOVA ($p < 0.05$).

the apoptosis, the TUNEL-LI and caspase 3 levels of LD-Si rats displayed the same distribution as the LD group, with higher values than those of ED rats.

3.7. Effect of silicon on antioxidant capacity

Fig. 4 shows the immunolocalization (Fig. 4A) and IRS of Cu/Zn-SOD, Mn-SOD, catalase, HO-1, and pNrf2 levels (Fig. 4B), the activities of the enzymes, SOD and catalase (Fig. 4C and D), levels of antioxidant mucosal status measured by the ORAC technique (Fig. 4E), nitrotyrosine (Fig. 4F) and colonic mucosa.

Cu/Zn-SOD, Mn-SOD, catalase and pNrf2 immunohistochemical levels of LD rats were lower than those of ED ones ($p < 0.01$). LD-Si rats showed significantly lower Cu/Zn-SOD and Mn-SOD levels compared to ED rats ($p < 0.001$) but higher levels than LD ones ($p < 0.001$), whilst catalase levels in LD-Si rats did not show significant differences compared with the other two groups. In the case of pNrf2, LD-Si rats only showed a significant increase compared to LD ones ($p < 0.001$). No significant differences of HO-1 levels in all the studied experimental groups were observed ($p > 0.05$). Considering enzymatic activities, the LD group showed higher catalase activity than the ED group ($p < 0.01$) and lower but not significant SOD activity. the LD-Si group displayed a significant increase in SOD activity compared to the other groups ($p < 0.001$). Additionally, LD-Si rats did not show significant differences in catalase activity compared to the ED group, but they exhibited a significant difference when compared to the LD group ($p < 0.01$). Lastly, the LD group showed the highest levels of ORAC among the others, being significantly different from the ED group ($p < 0.01$), but not from the LD-Si group, which did not differ from both. Regarding reactive nitrosamine species measured from nitrotyrosine, LD rats showed higher levels with respect to ED and LD-Si rats ($p = 0.0001$), while LD-Si rats showed significantly higher levels than ED rats ($p = 0.0001$).

3.8. Effect of the silicon glutathione redox system

Fig. 5 shows the glutathione redox system in colonic mucosa. Fig. 5A displays photographs showing the immunolocalization, while Fig. 5B presents the IRS of GPx and GR. Fig. 5C and D show the activities of GPx and GR, respectively. Fig. 5E depicts the levels of GSH and GSSG, along with the GSH/GSSG ratio.

Regarding the immunohistochemical levels of GPx and GR, LD rats displayed a decrease in the levels of both enzymes in comparison with ED ones ($p < 0.001$). LD-Si rats showed higher levels of GPx and GR with respect to LD rats ($p < 0.001$), without achieving the values of ED rats ($p < 0.001$). GPx activity was significantly lower in the LD-Si and LD groups compared to the ED group ($p < 0.001$) with no difference between LD-Si and LD. GR activity did not display significant differences between the three groups.

There were no differences in GSH levels among the three experimental groups ($p > 0.05$). Although GSSG levels were

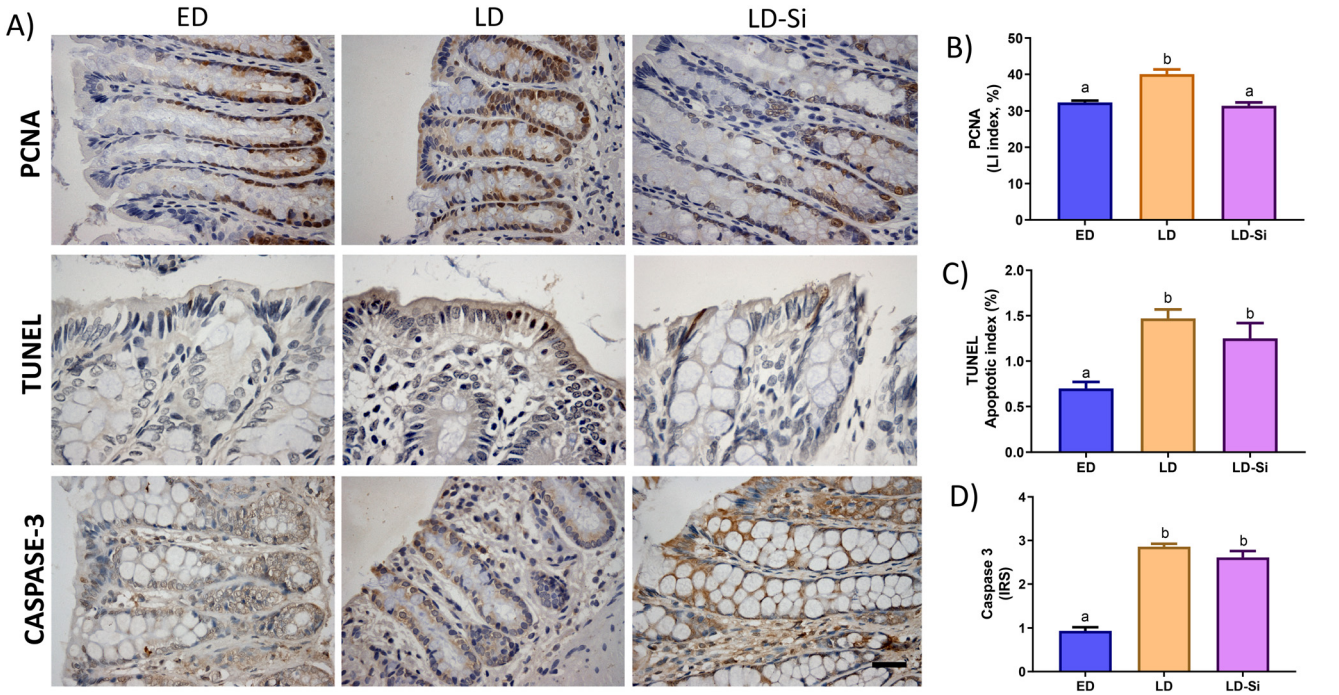

Fig. 3 Proliferation and apoptosis markers in early-stage diabetes (ED), late-stage diabetes (LD), and late-stage diabetes-silicon (LD-Si) groups. (A) Representative images of immunohistochemical labeling of PCNA, TUNEL and caspase 3, scale-bar: 50 μm, (B) proliferation index (PCNA-LI), (C) apoptotic index (TUNEL-LI), and (D) immunoreactivity scores of caspase-3. Values are expressed as mean ± SD. Different letters ($a < b < c$) indicate significant differences between groups, ANOVA ($p < 0.05$).

similar between LD and LD-Si groups, both were higher than those of the ED group. However, the GSH/GSSG ratio was lower in LD rats compared to that in ED rats, while in LD-Si rats the ratio increased significantly without reaching the values of ED rats.

3.9. Effect of silicon inflammatory parameters

Fig. 6 shows photographs of immunolocation of inflammation markers (Fig. 6A) and IRS of pNFkβ (Fig. 6B), TLR4 (Fig. 6C), TNFα (Fig. 6D), and IL-6 (Fig. 6E).

In every inflammatory marker, LD rats displayed higher levels than ED ones: pNFkβ ($p < 0.01$), TLR4 ($p < 0.001$), TNFα ($p < 0.001$), and IL-6 ($p < 0.001$). LD-Si showed intermediate levels compared to the other two groups with respect to TNFα ($p < 0.01$). However, regarding pNFkβ, TLR4, and IL-6, LD-Si rats displayed significantly lower levels than LD ones ($p < 0.001$), with no significant differences compared to the ED group.

3.10. Concurrence of colonic biomarkers

Colonic biomarker concurrence is displayed in Table 4 (ANOVA, $p < 0.05$). The GM index was highest in the ED group, with lower values in the LD-Si and LD groups. These two differed significantly from the ED group ($p = 0.03$) but not from each other. CM index and TJ index showed the highest values in the LD-Si group, differing significantly from ED ($p < 0.001$) and LD groups ($p < 0.001$). ED and LD rats did not show significant differences regarding the SCFA index, displaying higher levels than the LD-Si group, which differed significantly from both ED and LD groups ($p = 0.002$). Regarding the A&A index and GC index, the ED group showed the highest values among the three groups, followed by LD-Si ($p < 0.001$) and LD groups ($p < 0.001$), which were significantly different from each other.

3.11. Heatmap

Fig. 7 presents the correlation results of morphometric and faecal parameters, *F. prausnitzii*, *oxysterols*, *butyric and acetic acids*, antioxidant and inflammation markers and colonic marker concurrence scores.

Mucin production represented by the AB parameter as well as occludin levels showed negative correlations with the DTscore, and with 25-OHC, 27-OHC, and 7-OH oxysterols. On the other hand, PAS, AB and occludin showed positive correlations with all the colonic indexes except the SCFA index.

However, the balance between proliferation (PCNA) and apoptosis (TUNEL) exhibited contrasting correlations, showing positive association with DDscore, DTscore, faecal TBARS, and faecal cholesterol, as well as with the oxysterols 25-OHC, 27-OHC, 7-OH, and 7-OOH. In contrast, negative correlations were observed with butyric acid and the A&A index, GC index, and 24O HC.

F. prausnitzii along with butyric acid exhibited significant positive correlations with the activity of GPx and GSH/GSSG. In contrast, it showed negative correlations with the markers of the ROS/RNS balance, including ORAC and nitrotyrosine,

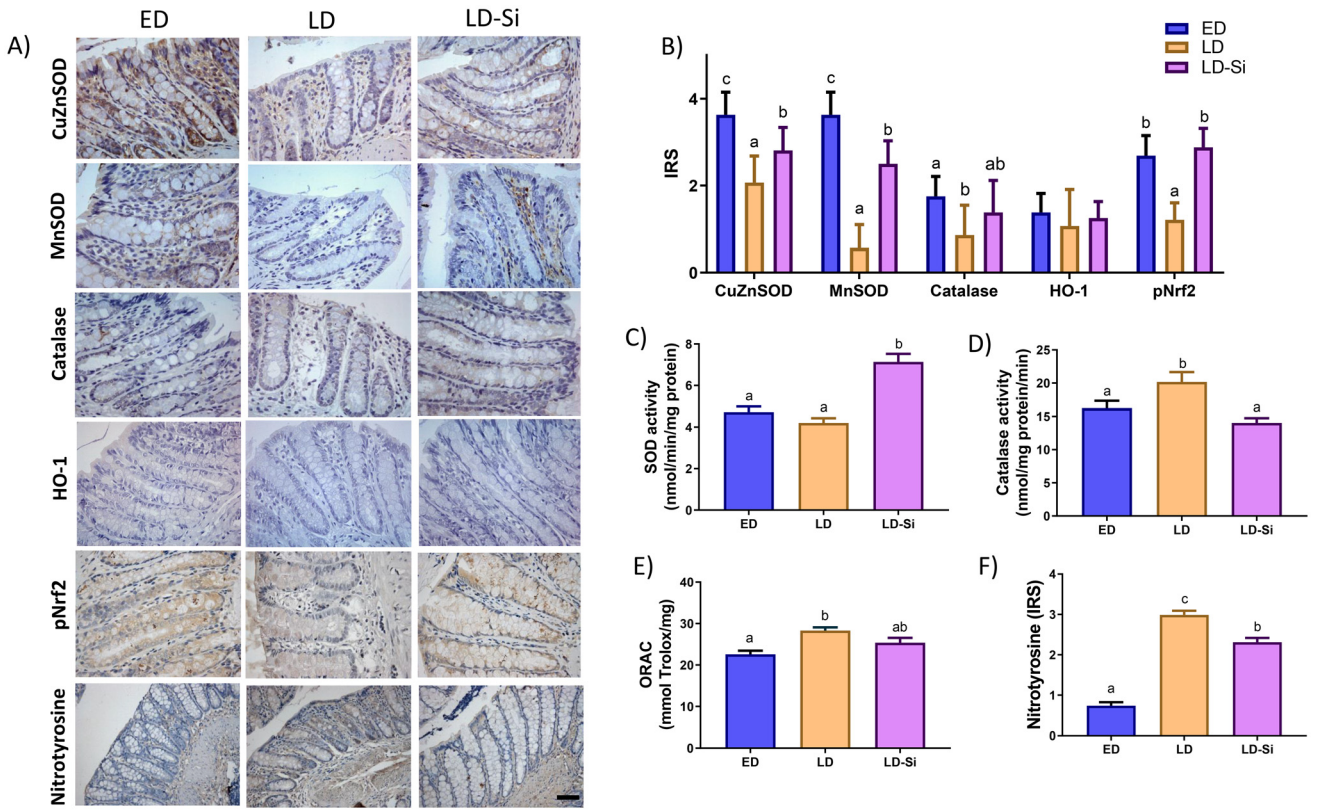

Fig. 4 Antioxidant enzymatic levels and concentrations, and ROS/RNS balance in early-stage diabetes (ED), late-stage diabetes (LD), and late-stage diabetes-silicon (LD-Si) groups. (A) Representative images of immunohistochemical labeling of CuZnSOD, MnSOD, catalase, HO-1, pNrf2 and nitrotyrosine antibodies, scale-bar: 50 μm, (B) immunoreactivity scores of CuZnSOD, MnSOD, catalase, HO-1 and pNrf2, (C) SOD activity (nmol min^{-1} mg^{-1} protein) and (D) catalase activity (nmol mg^{-1} protein per min); (E) ORAC (mmol Trolox mg^{-1}) and (F) immunoreactivity scores of nitrotyrosine. Values expressed as mean ± SD. Different letters ($a < b < c$) indicate significant differences between groups, ANOVA ($p < 0.05$).

TLR4, pNFkβ and the proinflammatory cytokines TNFα and IL-6.

Inflammation markers, including pNFκB, TLR4, TNFα, and IL-6, exhibited significant positive correlations with DTscore, DDscore, TBARS, and the oxysterols 25-OHC, 27-OHC, 7-OH, and 7-OOH. Conversely, they showed negative correlations with faecal silicon levels, *F. prausnitzii*, 5–6-EC, 24-OHC, and butyric acid, as well as with the TJ index, A&A index, and GC index.

4. Discussion

We have previously demonstrated that the consumption of Si-RM exerts hypoglycemic and hypolipidemic effects, improving the lipoprotein profile, cholesterol metabolism and the integrity of mucosal absorptive area in the proximal small intestine.[27,28,44] Given that altered cholesterol metabolism increases susceptibility to chemically induced colonic diseases, this article focuses on whether Si-RM consumption can reverse, at least partially, colonic mucosal disruption in rats with late-stage T2DM. For the first time, we report that silicon: (1) promotes a less toxic colonic luminal environment, evidenced by lower faecal lipoperoxidation and oxysterol levels; (2) improves the colonic mucosal epithelium by enhancing mucin secretion and reducing epithelial cell turnover; (3) enhances intestinal barrier function through upregulation of TJ, including occludin and ZO1; (4) induces antioxidant effects *via* activation of the Nrf2 pathway and improves the glutathione redox status; and (5) reduces colonic inflammation by lowering TNFα and IL-6 cytokine levels, likely through inhibition of the TLR4/NFκβp65 signalling pathway.

Firstly, we wanted to demonstrate that our late-stage T2DM rat model (LD group) has proven to reproduce the gut-derived typical metabolic alterations of diabetic dyslipidemia.[28,29] LD rats excreted high amounts of fat, cholesterol and pro-oxidants and pro-inflammatory oxysterols with a high degree of lipoperoxidation in faeces, which generated a potentially toxic environment in the distal colonic lumen. Autoxidation products of cholesterol are cytotoxic and may be useful markers of oxidative stress or for monitoring of the progression of various diseases.[45] This high concentration of luminal oxidized metabolites could be responsible for the disrupted colonic homeostasis found in LD rats compared to ED rats, characterized by gut microbiome alterations[42] and compromised barrier integrity.[28,44]

In relation to the dysbiosis and the changes in microbiota-derived SCFA production, LD rats showed a decrease of *F. prausnitzii* (butyrate-producing bacterium) and then lower

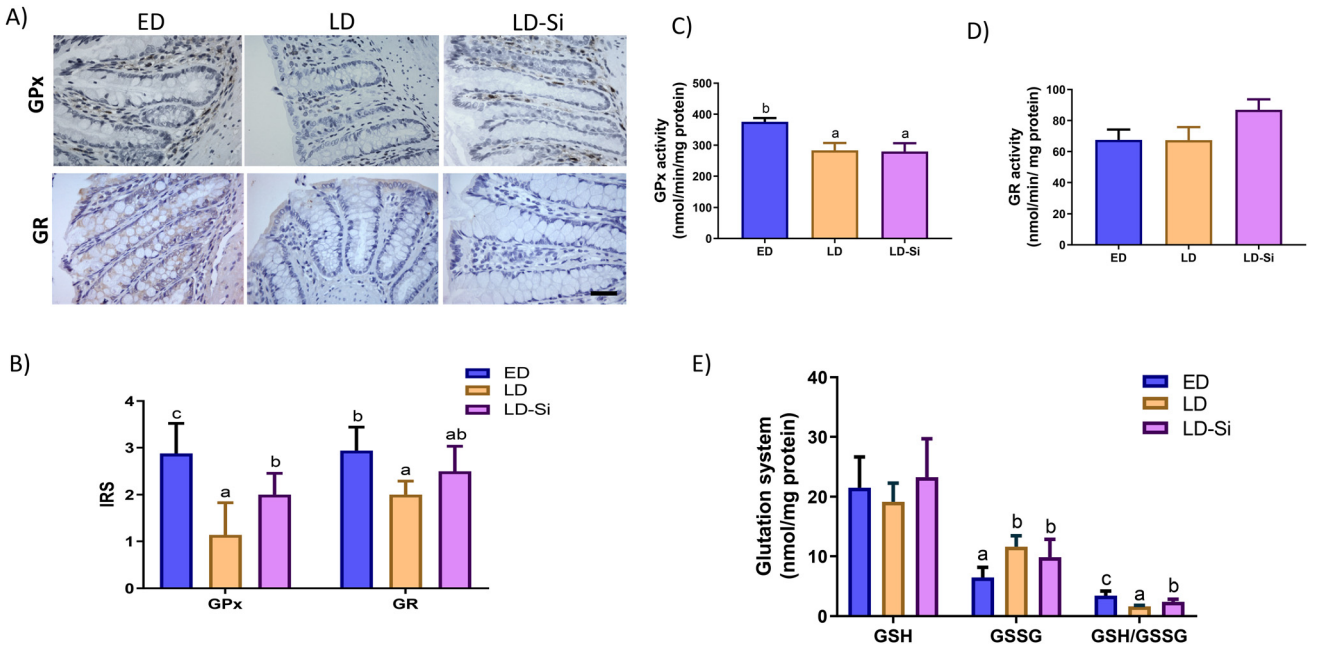

Fig. 5 Glutathione redox system in early-stage diabetes (ED), late-stage diabetes (LD), and late-stage diabetes-silicon (LD-Si) groups. (A) Representative images of immunohistochemical labeling of GPx and GR antibodies, scale-bar: 50 μm, (B) immunoreactivity scores of GPx and GR; (C) GPx and (D) GR activities (nmol min^{-1} mg^{-1} protein); and (E) glutathione system (nmol mg^{-1} protein): GSH, GSSG and GSH/GSSG ratio. Values expressed as mean ± SD. Different letters ($a < b < c$) indicate significant differences between groups, ANOVA ($p < 0.05$).

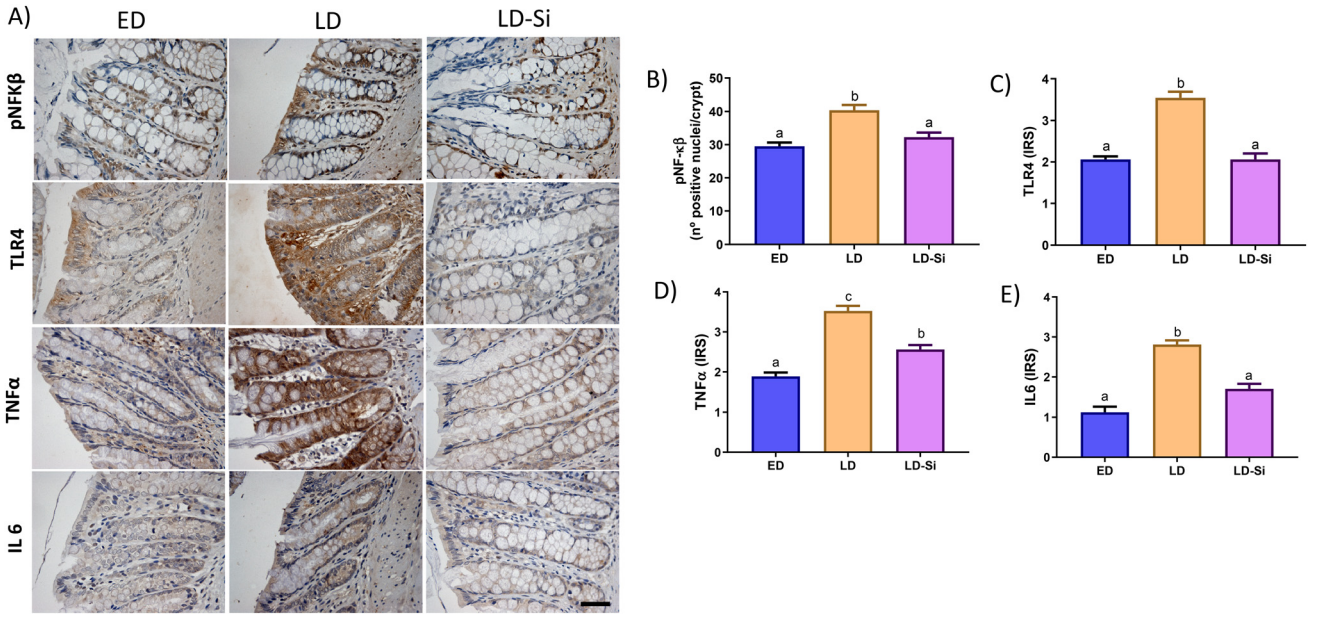

Fig. 6 Inflammation markers in early-stage diabetes (ED), late-stage diabetes (LD), and late-stage diabetes-silicon (LD-Si) groups. (A) Representative images of immunohistochemical labeling of pNFkβ, TLR4, TNFα and IL-6 antibodies; (B) pNFkβ (number of positive nuclei per crypt); (C) TLR4, (D) TNFα and (E) IL-6 immunoreactivity scores. Values expressed as mean ± SD. Different letters ($a < b < c$) indicate significant differences between groups using ANOVA ($p < 0.05$).

faecal butyrate content was found as observed in T2DM patients[46,47] and rats fed an atherogenic diet.[48] Specifically, this species has been associated with the ability of reducing intestinal permeability, leading to decreased endotoxin levels and improvements of glucose tolerance and systemic inflammation.[49] It had also been found that mice fed HSFHCD, or patients with obesity or T2DM, show an increased abundance of *Bacteroidetes* and *Proteobacteria*, and a lower abundance of

Table 4 Colonic marker concurrence of early-stage diabetes (ED), late-stage diabetes (LD) and late-stage diabetes-silicon (LD-Si) groups

	ED group	LD group	LD-Si group	*p*
GM index	9.43 ± 1.90^{c}	6.67 ± 2.10^{a}	7.67 ± 1.03^{b}	0.033
SCFA index	14.33 ± 1.25^{b}	13.00 ± 1.90^{b}	9.83 ± 0.98^{a}	0.002
CM index	11.50 ± 0.93^{b}	10.00 ± 0.76^{a}	14.63 ± 0.92^{c}	<0.001
TJ index	4.38 ± 0.74^{b}	2.38 ± 0.74^{a}	5.50 ± 0.76^{c}	<0.001
A&A index	$35.\ 75 \pm 1{,}58^{c}$	17.88 ± 1.73^{a}	29.5 ± 2.20^{b}	<0.001
GC index	75.17 ± 2.40^{c}	50.00 ± 4.80^{a}	67.33 ± 1.50^{b}	0.001

Values expressed as mean + SD (n = 8 per group). Labeled means in a row bearing different letters ($a < b < c$) were significantly different (at least $p < 0.05$ ANOVA followed by Scheffe or Tamhane *post-hoc* test). NS: no significant differences between groups. Gut microbiota index (GM index; *Bifidobacterium* spp., *F. prausnitzii*, *Lactobacillus* spp. and *Enterobacteriaceae*) was obtained considering the association of 4 species and their values calculated by adding the tertile value of each parameter (GM index range, 4 to 12); total SCFA index (ramified plus non-ramified fatty acids (SCFA index range, 6 to 18)); the colon morphology index, CM index (crypt depth, crypt density, positive goblet cells/crypt, PCNA index, and TUNEL index) (CM index range, 5 to 15); the TJ index was calculated adding tertile values of occludin plus ZO-1 (TJ index score range, 2 to 6); the antioxidant and anti-inflammatory index, A&A index (Mn-SOD + Cu/Zn-SOD + Catalase + GPx + GR + HO1 + pNrf2 + GSH/GSSG + ORAC + nitrotyrosine + TNFα + IL-6 + pNFkβ + TLR4) (A&A index range from 13 to 39), and the global colonic index (GC index), considering a conjoint marker of 17 variables obtained from the addition of tertile values of GM index + SCFA index + CM index + TJ index + A&A index (GC index range from 30 to 90).

Firmicutes and *Bifidobacteria.*[50,51] The limited changes observed between experimental groups in the gut microbiota in this study may be attributed to the fact that the ED group was already at the IR stage of T2DM. In this regard, it has been shown that the potential of the microbiota to produce SCFAs is already depleted in the early stages of diabetes.[52,53] Therefore, the richness and diversity of the intestinal microbiome to adapt to environmental changes were found to be diminished in T2DM, which reflected a decline in commensal bacteria such as *Firmicutes, Bacteroidetes, Lachnospiraceae*, and *Clostridium leptum.*[54,55] In addition, dysbiosis, along with impaired cholesterol and bile acid homeostasis, had been found to disrupt digestive, metabolic, and bacteriostatic functions, leading to dyslipidaemia and chronic low-grade inflammation, which are peculiar features of T2DM.[56]

Regarding disrupted colonic barriers, LD rats exhibited a disorganized mucosal layer structure, characterized by reduced crypt density, edema in the lamina propria, and inflammatory cell infiltration, indicating atrophy of the colonic mucosal wall. In parallel, dysfunction of the intestinal epithelium was observed in the mucosa of the LD group compared to that of the ED group. The number of goblet cells expressing mucin glycoprotein, as assessed by PAS and AB staining, decreased—goblet cells are critical for forming the mucus layer that protects and lubricates the colonic epithelial surface. A thinner mucus layer with reduced contents of bicarbonate, glycoproteins, antimicrobials, IgA, and antioxidants makes the intestinal barrier more vulnerable to bacteria, luminal toxins, and pro-oxidative molecules, resulting in enterocyte damage and loss of intestinal barrier integrity.[57,58] Furthermore, an increased epithelial cell turnover was observed in LD rats, suggesting a compensatory mechanism to address mucosal atrophy. The coordinated proliferation and migration of colonic epithelial cells are essential for maintaining barrier function and facilitating epithelial restitution following injury.[59] Additionally, LD rats exhibited significantly lower levels of TJ, including occludin and ZO-1, compared to control ED rats, indicating alterations in the colonic barrier, which have been correlated with intestinal hyperpermeability. Based on our study results, it is confirmed that luminal ROS from atherogenic diets predisposed the intestine to chronic diseases such as T2DM, primarily through disruption of the gut barrier function, *via* alteration in the enterocyte shedding–proliferation axis and disruption of the ocludin-ZO1 pathway.[60]

Furthermore, we also found that the colonic mucosa of LD rats exhibited reduced antioxidant and GSH-dependent detoxification capacity, contributing to mucosal damage. This was accompanied by increased pro-inflammatory cytokines and TLR4/NF-κB pathway activation, processes that play a central role in intestinal barrier dysfunction in T2DM.[17] Additionally, oxysterols like 7-OHC and 25-OHC impair intestinal barrier integrity and trigger pro-inflammatory immune responses.[14] Dysbiosis-induced LPS accumulation further activates TLR4/NF-κB signaling, driving inflammation and insulin resistance (IR) *via* adipocytes and macrophages.[61,62] This disrupted colonic homeostasis, likely linked to pro-inflammatory cytokines from gut-associated lymphoid tissue (GALT), exacerbates systemic inflammation in T2DM.[7] Additionally, pro-inflammatory cytokines and bacterial toxins contribute to mitochondrial dysfunction, further compromising intestinal barrier integrity and gut–liver axis homeostasis, key drivers of T2DM progression.[63] The defective intestinal barrier detected in LD rats could enhance transepithelial flux, facilitating translocation of luminal toxins into the systemic circulation, leading to metabolic endotoxemia and T2DM progression.[64,65] These results suggest that the impairment of the intestinal barrier, triggered by the toxic luminal environment in the colon, may be a contributing factor in the progression of T2DM pathogenesis of LD rats. Consequently, reducing metabolic endotoxemia by improving gut barrier integrity could represent a promising strategy for treating diabetic dyslipidemia.

On the other hand, Si-RM consumption modified the composition of the colonic lumen content, thereby affecting the mucosal barrier. Our previous studies have shown that one of the mechanisms through which silicon exerts a cholesterol-lowering effect is by activating luminal and intestinal transepithelial cholesterol efflux (TICE) by upregulation of LXRα/β, LDLr and ABCG5/8 transporter levels in the small intestine, leading to increased faecal fat and cholesterol excretion.[27,28] Despite the higher fat and cholesterol contents in faeces of LD-Si rats, the large amount of silicon in the intestinal lumen promoted a less oxidized luminal colonic environment. The oxysterols present in faeces, either from enzymatic transformation of cholesterol or ROS induction, were reduced in LD-Si rats compared to LD rats, including 25OHC (68.50%, $p <$

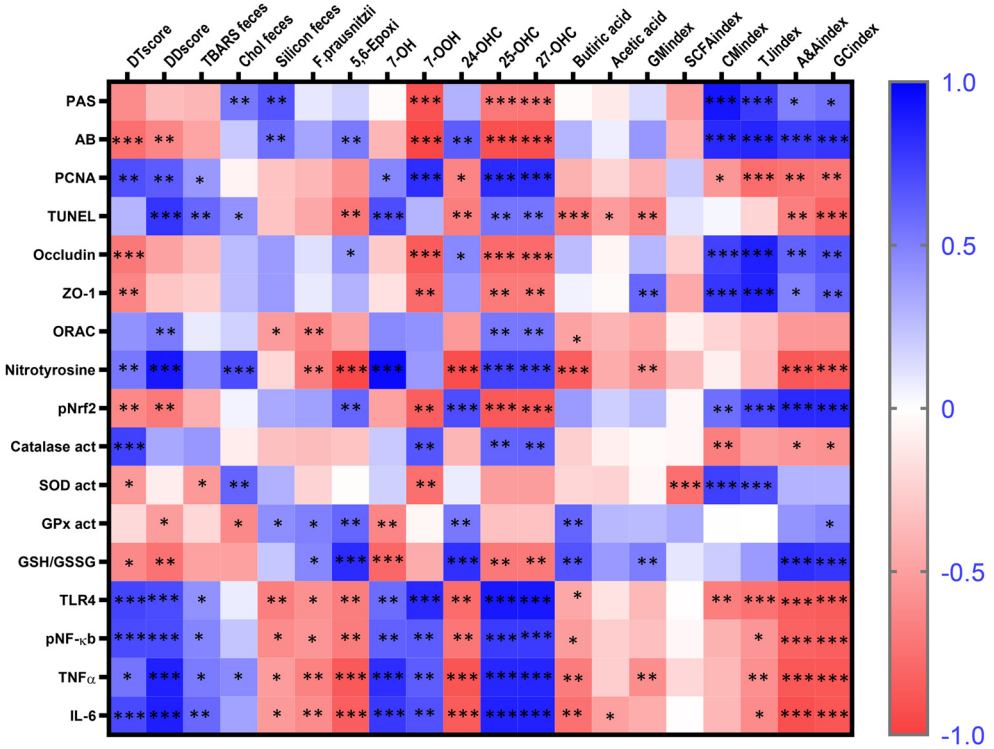

Fig. 7 Association between morphometric, microbiota, short-chain fatty acid, oxysterol, antioxidant and inflammation markers and scores. Pearson or Spearman correlation values were used for the matrix. The color intensity of the heatmap represents the association degree: blue, positive association; orange, negative association. *Denotes adjusted $p < 0.05$, ** $p < 0.01$, and *** $p < 0.001$. The parameters displayed in the heatmap are PAS, AB, PCNA, TUNEL, occludin, ZO-1, ORAC, nitrotyrosine, pNrf2, catalase activity, SOD activity, GPx activity, GSH/GSSG, TLR4, pNF-Kβ, TNFα, IL-6, DTscore (insulin + glucose + HOMA–β), DDscore (cholesterol + triglycerides + atherogenic index), faecal TBARS, faecal cholesterol, faecal silicon, *F. prausnitzii*, 5,6-EC, 7-OH, 7-OOH, 24-OHC, 25-OHC, 27-OHC, butyrate, acetate, GM index (*Bifidobacterium* spp. + *F. prausnitzii* + Lactobacillus spp. + *Enterobacteriaceae*), SCFA index (acetate + propionate + butyrate + isobutirate + valerate and isovalerate), CM index (crypt depth + crypt density + positive goblet cells/crypt + PCNA index + TUNEL index), TJ index (occludin + ZO-1), A&A index (Mn-SOD + Cu/Zn-SOD + catalase + GPx + GR + HO1 + pNrf2 + GSH/GSSG + nitrotyrosine + TNFα + IL-6 + pNFkβ +TLR4), and GC index (GM index + SCFA index + CM index + TJ index + A&A index).

0.0001), 27OHC (69.11%, $p < 0.0001$), 7OHC (15.55%, $p < 0.01$) and 7OOHC (28.58%, $p < 0.001$). This reduction could help prevent the increase in lipoperoxidation of fecal content, as indicated by lower TBARS values ($p < 0.05$). However, silicon also modulated the metabolism of other oxysterols by promoting the biotransformation of cholesterol into more polar compounds to facilitate their elimination, increasing the excretion of 24-OHC and 5,6-EC. This increased faecal excretion by silicon could prevent the arterial intima accumulation of 24S-OHC and 5,6-EC, thereby improving advanced atherosclerotic disease and systemic inflammatory activity, as has been observed in individuals with severe hyperlipidemia.[66,67] Specifically, the increased excretion of 24-OHC oxysterol, an oxysterol produced enzymatically by CYP46A1 to regulate cholesterol catabolism in the brain, could help prevent its neurotoxicity.[68] In this study, faecal oxysterol levels were significantly correlated with both DTscore and DSscore, which reflect the stage of T2DM progression, and may act as feedback regulators of cholesterol synthesis.

In addition to oxysterol content, the colon lumen is rich in microbial metabolites and fermentation products produced by the microbiota, which were also altered in LD rats. However, despite the increased excretion of fat and cholesterol, LD-Si rats did not show greater dysbiosis. This may be because by the time they start consuming Si-RM at the fourth week, the microbiota would already be altered, making it difficult to reverse this disruption within the context of an HSFHCD. Si-RM consumption did not modify the diversity of the microbiota with respect to LD rats, maintaining a lower relative abundance of *F. prausnitzii* bacteria and consequently, lower butyrate levels, with respect to the ED group. However, the GM index (a useful bacterial index calculated from the association of four species of faeces, that is, *Bifidobacterium* spp., *F. prausnitzii, Lactobacillus* spp. and *Enterobacteriaceae*) increased in LD-Si rats compared to that in LD rats, although it did not reach the values of ED rats. Since there were no significant changes in the microbiota, there were only minor changes in SCFA levels. This suggests that silicon helped in preventing significant disruption of the microbiota and SCFA production, despite the substantial excretion of fat in the faeces. We only found that silicon led to a further reduction in acetate content in the faeces, which could explain the lower

SCFA production, as indicated by the SCFA index, compared to both LD and ED groups. A reduced concentration of acetate in the colon could be due to an increase in its absorption, leading to higher serum acetate levels, which could have beneficial effects on peripheral tissues, such as stimulating pancreatic β-cell proliferation to induce greater insulin secretion.[69,70] Moreover, we found correlations between acetate levels and faecal contents of 24-OHC and 5,6-EC, which could explain the indirect beneficial effects of silicon through these metabolites at the systemic level. On the other hand, we have previously postulated that silicon in the luminal compartment could also act by interacting with micellar composition, reducing intestinal cholesterol absorption[27,28] and sequestering metabolic byproducts for excretion.[71] The increase in fecal weight and moisture following silicon supplementation could be attributed to this property, which enhances water retention in the intestinal lumen, resulting in softer and bulkier stools. This, in turn, would lead silicon to modulate gut motility and act as a mild osmotic agent, promoting water influx into the colon, reducing its reabsorption, and increasing stool hydration. We could consider that silicon may exert a fiber-like effect by altering nutrient digestibility and bile acid binding, leading to a greater amount of undigested material in the feces.

These changes towards a less toxic luminal content induced by Si-RM consumption exerted a multifaceted adaptive improvement in the colonic mucosal barrier. Silicon promoted higher density and depth crypts, as well as a better organized mucosal layer structure compared to those of LD rats. A growing body of evidence suggests the direct involvement of silicon in the synthesis of the extracellular matrix and/or its stabilization, particularly in the case of collagen, a key structural protein of connective tissues and the intestinal lamina propria of the colonic mucosa.[72] However, we did not observe any increase in the silicon content in the mucosa of the cecum,[41] suggesting that the effects of dietary silicon on the colonic wall are likely mediated from the intestinal lumen.

Silicon also affected the homeostasis of the intestinal epithelium. Si-RM consumption reduced reactive epithelial hyperproliferation found in LD rats. According to our previous studies on the small intestine,[27,28] silicon slowed down epithelial cell turnover by decreasing PCNA-LI, with no changes in apoptosis, measured by TUNEL-LI and caspase-3 levels. The improved proliferation/apoptosis balance of epithelial cells was directly associated with faecal contents of 25-OHC, 27-OHC, and 7-OHC, while being inversely correlated with 24-OHC, 5,6-EC, and butyrate levels. However, apoptosis was positively correlated with faecal fat content and TBARS levels, and negatively correlated with microbiota diversity, specifically *F. prausnitzii* and *Bifidobacterium* spp., as indicated by the strong correlation between these factors. Dietary silicon directly inhibited proliferation and promoted apoptosis in transformed cells, suggesting a potential strategy for preventing complications associated with metabolic diseases, such as colon cancer.

Simultaneously, silicon increased the number of PAS and AB goblet cells and enhanced the mucus layer components, thereby protecting the mucus barrier function. The restoration of the mucus layer was directly induced by faecal silicon content (PAS, $r = 0.806$, $p = 0.0001$; AB, $r = 0.717$, $p = 0.001$), blocking the inhibitory effect on the mucin production by excessive amounts of fat and cholesterol present in faeces of LD-Si rats. Mucin proteins, produced by goblet cells, play a crucial role in enhancing the integrity of the intestinal barrier, being essential elements of the gut's biochemical defence system against microbes.[73] The higher amounts of proteoglycans secreted by goblet cells can participate in microbial defence[74] and protect the intestinal mucosa through the non-covalent binding of its glycosyl to the glycosyl groups of bacteria.[75] However, no correlation between PAS/AB cells and microbiota has been found in this study. The increase in the mucus layer induced by silicon could help protect the intestinal epithelium from bacteria and their metabolites, preventing intestinal permeability and the translocation of bacterial components, such as LPS, into the systemic circulation, thereby mitigating metabolic endotoxemia.[76]

Furthermore, Si-RM consumption mitigated the reduction in TJ levels of occludin and ZO-1, thereby improving intestinal barrier integrity and reducing colonic permeability. The modulation of TJs by silicon was influenced by the oxidative status of luminal oxysterols, as reflected by the TJ index. This index was positively correlated with faecal silicon, 24-OHC, and 5,6-EC contents, and negatively correlated with faecal 25-OHC, 27-OHC, 7-OHC, and 7-OOH levels. We also observed a strong association between the markers of mucosal barrier integrity, namely CM index and TJ index, and metabolic parameters, such as DTscore and DSscore, indicating that mucosal integrity was closely linked to the stage of diabetic dyslipidemia. Notably, PCNA-LI levels were negatively correlated with TJ index, suggesting an efficient adaptation to cellular demands by regulating the sealing and opening of the paracellular transport pathways under dyslipidemic and T2DM conditions.[77] Collectively, these effects of Si-RM consumption contributed to the preservation of the intestinal barrier, thereby preventing progression to a more advanced stage of T2DM. This was evidenced by improved histopathological outcomes and markers of intestinal epithelium homeostasis, including the proliferation/apoptosis balance, goblet cell density, and TJ integrity.

The excess of reactive oxygen and nitrogen species (ROS/RNS) under pathological conditions, along with the subsequent loss of redox homeostasis, can contribute to the progression and complications of T2DM. The ability of silicon to enhance colonic barrier integrity may be linked to its antioxidant and anti-inflammatory properties.[26,78] As anticipated, Si-RM intake significantly reduced RNS, as indicated by nitrotyrosine levels, and showed a tendency to decrease ROS absorbance capacity, measured by the ORAC technique. To improve the oxidative state in the colon, silicon exerted a protective effect by activating the Nrf2/Keap1/ARE signalling pathway, which is well recognized for its role in regulating antioxidant enzyme expression.[79] Nrf2 has also been associated with enhanced expression of epithelial TJ and the maintenance of intestinal barrier integrity,[80] while concurrently decreasing

apoptotic and inflammatory factors.[81] We observed that the phosphorylation of Nrf2 at serine[42] activated MnSOD and Cu/ZnSOD levels, as well as SOD activity, with no changes in catalase and GPx activities, or HO-1 levels in the mucosa of LD-Si rats compared to those of LD rats, resulting in values similar to those of the ED group. The SOD enzyme catalyses the dismutation of superoxide radicals ($O2^{\bullet}-$) into hydrogen peroxide, which functions as a signalling molecule mediating various biological responses such as cell proliferation, differentiation, and migration.[82] This mechanism may indirectly modulate silicon's effect on colonic mucosal integrity. Consistent with this, the significant relationship found between the TJ index, CM index, pNrf2, MnSOD levels, and SOD and CAT activities supported this hypothesis ($p < 0.001$). Moreover, the higher GSH : GSSG ratio, along with increased GPx and GR activities, suggested that Si-RM intake promoted a pro-reductive shift in the colonic mucosa. CM index was directly correlated with GSH levels ($r = 0.442$, $p = 0.032$) and GR activity ($r = 0.475$, $p = 0.019$), indicating a parallel improvement in the glutathione redox system and colonic mucosal integrity.[83] Accordingly, silicon-containing water intake induced antioxidant effects and provided gastrointestinal protection against gastric damage caused by pylorus ligation in rodents.[84]

Additionally, silicon was able to attenuate intestinal inflammatory processes by targeting the TLR4/NF-κB pathway and reducing the production of pro-inflammatory cytokines, including IL-6 and TNF-α, in the colonic mucosa. Furthermore, the impact of faecal components on the colonic lumen influenced both the antioxidant defence system and the inflammatory state of the colonic mucosa. ORAC, nitrotyrosine, GSSG, TLR4, pNF-κB, TNF-α, and IL-6 levels in the colonic mucosa were inversely correlated with 24-OHC and 5,6-EC contents, whereas positive relationships were observed with faecal 25-OHC, 27-OHC, and 7-OHC levels. The reduced content of 25-OHC and 27-OHC induced by silicon in the lumen may contribute to their antioxidant and anti-inflammatory effects.[67] Specifically, 25-OHC promotes the production of pro-inflammatory cytokines and chemokines such as TNF-α, IL-6, and IL-8, while also inhibiting the secretion of the anti-inflammatory factor IL-10.[85] It has also been shown that the inflammatory cytokine TNF-α increases epithelial permeability by altering TJ function, structure, and dynamics.[86] The reduction of 25-OH explains the lower release of cytokines and, consequently, the improved TJ protein levels found in LD-Si rats.

Despite the limited impact of silicon on microbiota and its metabolites, emerging evidence suggests that the interaction between the gut bacteria and intestinal epithelial cells exerts protective effects by regulating the redox status, thereby contributing to colonic homeostasis.[87] In this regard, *F. prausnitzii* displayed an inverse correlation with TLR4, pNFκβ, TNF-α, and IL-6 levels, while microbiota diversity, as represented by GM index, was correlated with ORAC, nitrotyrosine, GSH/GSSG ratio, and MnSOD and CuZnSOD levels. However, the SCFA index appeared to be independent of antioxidant and inflammatory markers. The A&A index, which reflects both antioxidant and anti-inflammatory markers, was directly associated with acetate and butyrate levels, as well as with *F. prausnitzii* abundance, and inversely correlated with faecal fat and cholesterol contents and TBARS. Collectively, these findings suggest that Si-RM consumption modulated the antioxidant enzyme system *via* Nrf2 activation, along with an increase in the cellular GSH : GSSG ratio, shifting the redox environment toward a more reducing state. Furthermore, silicon modulated the TLR4/NF-κB pathway and reduced the production of pro-inflammatory cytokines, such as IL-6 and TNF-α, thereby mitigating inflammation in the colonic mucosa. These effects likely contributed to improved mitochondrial function, supporting intestinal homeostasis and metabolic health.

The silicon-induced upregulation of TJ and the improvement in intestinal mucosal barrier integrity likely prevented the excessive translocation of endotoxins and noxious agents into the bloodstream, attenuating the activation of local and systemic inflammatory responses[51] and slowing the progression of T2DM in LD-Si rats. These findings suggest that silicon, by regulating oxidative stress and inflammation, enhances mechanisms that drive mitochondrial bioenergetics and helps maintain intestinal barrier integrity and stability.[63] Given these properties, silicon could be a promising antioxidant candidate for nutritional adjuvant therapy in managing T2DM progression and diabetic dyslipidemia.

Finally, the combination of selected bacterial genera/species (GM index), ramified and non-ramified fatty acids (SCFA index), colonic morphology markers (CM index), TJ (TJ index), and antioxidant and anti-inflammatory markers (AA index) contributed to the formulation of a global colonic score (GC index), which effectively differentiated the colonic health status across the experimental groups.[42] The LD-Si rats exhibited a higher GC index compared to the LD rats, with values approaching those of the ED rats. The positive correlation observed between GC index and DTScore and DSscore further demonstrated the ability of silicon to reverse colonic mucosal alterations and slow down the progression of T2DM.

These results support the nutritional potential of Si-RM as a functional food, highlighting its role as a dietary intervention that enhances gut barrier function, reduces inflammation, and supports metabolic homeostasis. However, some limitations of the study must be noted: (1) only a limited number of bacterial species/genera were analysed in the gut microbiota; (2) plasmatic oxysterol and SCFA levels were not assessed; (3) the gut microbiota produces a wide array of metabolites, such as LPS, bile acids, and amino acid derivatives, which may also play crucial signalling roles; (4) a healthy control group and groups treated with antidiabetic drugs were not included in the study; and (5) silicon intake as a preventive nutritional supplement could also be explored. Despite these limitations, the findings provide new insights into intestinal mechanisms involved in T2DM progression, particularly using a late-stage T2DM rat model, and suggest that Si-RM could be incorporated into nutritional adjuvant strategies for managing T2DM and related metabolic disorders.

5. Conclusions

In conclusion, Si-RM consumption in late-stage T2DM offers several beneficial local effects in the colon, including detoxification of luminal oxysterols, enhancement of colonic barrier integrity, improved antioxidant capacities, and reduced inflammation. These results suggest that silicon, as a functional ingredient in meat, could be a valuable nutritional adjuvant strategy for mitigating the progression and complications of T2DM, particularly by maintaining gut health.

Author contributions

M. H-M: conceptualization, investigation, data curation, formal analysis, visualization, writing original draft, and review & editing; A. B: formal analysis, visualization, and writing original draft; A.G: conceptualization, methodology, investigation, and supervision; R. R-C: formal analysis; A. M-G: conceptualization, data curation, and formal analysis; L.A.: formal analysis; R.A.G-F: data curation and formal analysis; S. B: project administration, funding acquisition, and resources. J. B: project administration, funding acquisition, and supervision; FJ. S–M: project administration, funding acquisition, and supervision; ME. L-O: conceptualization, data curation, formal analysis, visualization, writing – original draft, writing – review & editing, and supervision.

Data availability

Data for this article, including supplementary materials, are available at: **https://drive.google.com/file/d/1xerxIXrjfQh5UMKj0wyJNzYqfAxoVkPZ/view?usp=drive_link**.

The data supporting this article have been included as part of the ESI.†

Conflicts of interest

The authors declare no conflicts of interest. The funders had no role in the design of the study; in the collection, analyses, or interpretation of data; in the writing of the manuscript; or in the decision to publish the results.

Acknowledgements

This work was supported by the Spanish Projects with references AGL2014–53207-C2–2-R and PR75/18–21603 Santander-UCM Project and PID2019–103872RB-I00 and /AEI/10.13039/501 100 011 033. Rocío Redondo–Castillejo was supported by grant FPU20/0 2920 from the Spanish Ministry of Universities. We thank Dr. María José González-Muñoz for her scientific assessment. Special thanks go to Christopher Mulhern for editing the English language manuscript. None of the authors received reimbursement, honoraria, or stipends for their participation in the development of these experiments. The research was designed, executed, analysed and communicated only by the authors of this work.

References

1 S. Jiang, H. Liu and C. Li, Dietary Regulation of Oxidative Stress in Chronic Metabolic Diseases, *Foods*, 2021, **10**, 1854.
2 P. Zhang, T. Li, X. Wu, E. C. Nice, C. Huang and Y. Zhang, Oxidative stress and diabetes: antioxidative strategies, *Front. Med.*, 2020, **14**, 583–600.
3 M. Lytrivi, A. L. Castell, V. Poitout and M. Cnop, Recent Insights Into Mechanisms of β-Cell Lipo- and Glucolipotoxicity in Type 2 Diabetes, *J. Mol. Biol.*, 2020, **432**, 1514–1534.
4 T. Hiyoshi, M. Fujiwara and Z. Yao, Postprandial hyperglycemia and postprandial hypertriglyceridemia in type 2 diabetes, *J. Biomed. Res.*, 2019, **33**, 1.
5 T. Liu, L. Zhang, D. Joo and S. C. Sun, NF-κB signaling in inflammation, *Signal Transduction Targeted Ther.*, 2017, **2**, 17023.
6 M. C. Arkan, A. L. Hevener, F. R. Greten, S. Maeda, Z. W. Li, J. M. Long, A. Wynshaw-Boris, G. Poli, J. Olefsky and M. Karin, IKK-beta links inflammation to obesity-induced insulin resistance, *Nat. Med.*, 2005, **11**, 191–198.
7 F. Di Vincenzo, A. Del Gaudio, V. Petito, L. R. Lopetuso and F. Scaldaferri, Gut microbiota, intestinal permeability, and systemic inflammation: a narrative review, *Intern. Emerg. Med.*, 2024, **19**, 275–293.
8 R. B. Oliveira, L. P. Canuto and C. B. Collares-Buzato, Intestinal luminal content from high-fat-fed prediabetic mice changes epithelial barrier function in vitro, *Life Sci.*, 2019, **216**, 10–21.
9 M. W. Rohr, C. A. Narasimhulu, T. A. Rudeski-Rohr and S. Parthasarathy, Negative Effects of a High-Fat Diet on Intestinal Permeability: A Review, *Adv. Nutr.*, 2020, **11**, 77–91.
10 X. Zhang, O. O. Coker, E. S. H. Chu, K. Fu, H. C. H. Lau, Y. X. Wang, A. W. H. Chan, H. Wei, X. Yang, J. J. Y. Sung and J. Yu, Dietary cholesterol drives fatty liver-associated liver cancer by modulating gut microbiota and metabolites, *Gut*, 2021, **70**, 761–774.
11 M. D. Carretta, J. Quiroga, R. López, M. A. Hidalgo and R. A. Burgos, Participation of Short-Chain Fatty Acids and Their Receptors in Gut Inflammation and Colon Cancer, *Front. Physiol.*, 2021, **12**, 662739.
12 F. A. de Freitas, D. Levy, C. O. Reichert, E. Cunha-Neto, J. Kalil and S. P. Bydlowski, Effects of Oxysterols on Immune Cells and Related Diseases, *Cells*, 2022, **11**(8), 1251.
13 O. Guillemot-Legris, V. Mutemberezi and G. G. Muccioli, Oxysterols in Metabolic Syndrome: From Bystander Molecules to Bioactive Lipids, *Trends Mol. Med.*, 2016, **22**, 594–614.
14 T. Willinger, Oxysterols in intestinal immunity and inflammation, *J. Intern. Med.*, 2019, **285**, 367–380.
15 P. D. Cani, J. Amar, M. A. Iglesias, M. Poggi, C. Knauf, D. Bastelica, A. M. Neyrinck, F. Fava, K. M. Tuohy,

C. Chabo, A. Waget, E. Delmée, B. Cousin, T. Sulpice, B. Chamontin, J. Ferrières, J. F. Tanti, G. R. Gibson, L. Casteilla, N. M. Delzenne, M. C. Alessi and R. Burcelin, Metabolic endotoxemia initiates obesity and insulin resistance, *Diabetes*, 2007, **56**, 1761–1772.

16 Y. C. Lu, W. C. Yeh and P. S. Ohashi, LPS/TLR4 signal transduction pathway, *Cytokine*, 2008, **42**, 145–151.

17 K. Gil-Cardoso, I. Ginés, M. Pinent, A. Ardévol, X. Terra and M. Blay, A cafeteria diet triggers intestinal inflammation and oxidative stress in obese rats, *Br. J. Nutr.*, 2017, **117**, 218–229.

18 A. Szilagyi, Relationship(s) between obesity and inflammatory bowel diseases: possible intertwined pathogenic mechanisms, *Clin. J. Gastroenterol.*, 2020, **13**, 139.

19 R. Farré, M. Fiorani, S. A. Rahiman and G. Matteoli, Intestinal Permeability, Inflammation and the Role of Nutrients, *Nutrients*, 2020, **12**(4), 1185.

20 U. Hammerling, J. Bergman Laurila, R. Grafström and N. G. Ilbäck, Consumption of Red/Processed Meat and Colorectal Carcinoma: Possible Mechanisms Underlying the Significant Association, *Crit. Rev. Food Sci. Nutr.*, 2016, **56**, 614–634.

21 C. Li, T. R. P. Bishop, F. Imamura, S. J. Sharp, M. Pearce, S. Brage, K. K. Ong, H. Ahsan, M. Bes-Rastrollo, J. W. J. Beulens, N. den Braver, L. Byberg, S. Canhada, Z. Chen, H. F. Chung, A. Cortés-Valencia, L. Djousse, J. P. Drouin-Chartier, H. Du, S. Du, B. B. Duncan, J. M. Gaziano, P. Gordon-Larsen, A. Goto, F. Haghighatdoost, T. Härkänen, M. Hashemian, F. B. Hu, T. Ittermann, R. Järvinen, M. G. Kakkoura, N. Neelakantan, P. Knekt, M. Lajous, Y. Li, D. J. Magliano, R. Malekzadeh, L. Le Marchand, P. Marques-Vidal, M. A. Martinez-Gonzalez, G. Maskarinec, G. D. Mishra, N. Mohammadifard, G. O'Donoghue, D. O'Gorman, B. Popkin, H. Poustchi, N. Sarrafzadegan, N. Sawada, M. I. Schmidt, J. E. Shaw, S. Soedamah-Muthu, D. Stern, L. Tong, R. M. van Dam, H. Völzke, W. C. Willett, A. Wolk, C. Yu, N. G. Forouhi and N. J. Wareham, Meat consumption and incident type 2 diabetes: an individual-participant federated meta-analysis of 1·97 million adults with 100 000 incident cases from 31 cohorts in 20 countries, *Lancet Diabetes Endocrinol.*, 2024, **12**, 619–630.

22 F. José Sánchez-Muniz, M. José González-Muñoz, A. Macho-González, J. Benedí, A. Garcimartín, E. López-Oliva, J. A. Santos-López, S. Bastida and en representación del grupo AFUSAN, Cuando el silicio transmuta en oro, *Journal of Negative and No Positive Results*, 2020, **5**, 202–211.

23 M. Hernández-Martín, A. Macho-González, A. Garcimartín, M. E. López-Oliva, A. Bocanegra, R. Redondo-Castillejo, S. Bastida, J. Benedí and F. J. Sánchez-Muniz, Silicon-enriched meat positively improves plasma lipidaemia and lipoproteinaemia, LDLr, and insulin capability and the signalling pathway induced by an atherogenic diet in late-stage type 2 diabetes mellitus rats, *Food Funct.*, 2024, **15**, 1513–1526.

24 M. Hernández-Martín, A. Garcimartín, A. Bocanegra, R. Redondo-Castillejo, C. Quevedo-Torremocha, A. Macho-González, R. A. G. Fernández, S. Bastida, J. Benedí, F. J. Sánchez-Muniz and M. E. López-Oliva, Silicon as a Functional Meat Ingredient Improves Jejunal and Hepatic Cholesterol Homeostasis in a Late-Stage Type 2 Diabetes Mellitus Rat Model, *Foods*, 2024, **13**, 1794.

25 M. Hernández-Martín, A. Bocanegra, R. Redondo-Castillejo, A. Macho-González, F. J. Sánchez-Muniz, J. Benedí, S. Bastida, R. A. García-Fernández, A. Garcimartín and M. E. López-Oliva, Could Duodenal Molecular Mechanisms be Involved in the Hypocholesterolemic Effect of Silicon Used as Functional Ingredient in Late-Stage Type 2 Diabetes Mellitus?, *Mol. Nutr. Food Res.*, 2022, **66**(24), e2200104.

26 J. A. Santos-López, A. Garcimartín, P. Merino, M. E. López-Oliva, S. Bastida, J. Benedí and F. J. Sánchez-Muniz, Effects of Silicon vs. Hydroxytyrosol-Enriched Restructured Pork on Liver Oxidation Status of Aged Rats Fed High-Saturated/High-Cholesterol Diets, *PLoS One*, 2016, **11**(1), e0147469.

27 M. Hernández-Martín, A. Bocanegra, R. Redondo-Castillejo, A. Macho-González, F. J. Sánchez-Muniz, J. Benedí, S. Bastida, R. A. García-Fernández, A. Garcimartín and M. E. López-Oliva, Could Duodenal Molecular Mechanisms be Involved in the Hypocholesterolemic Effect of Silicon Used as Functional Ingredient in Late-Stage Type 2 Diabetes Mellitus?, *Mol. Nutr. Food Res.*, 2022, **66**(24), e2200104.

28 M. Hernández-Martín, A. Garcimartín, A. Bocanegra, R. Redondo-Castillejo, C. Quevedo-Torremocha, A. Macho-González, R. A. García-Fernández, S. Bastida, J. Benedí, F. J. Sánchez-Muniz and M. E. López-Oliva, Silicon as a Functional Meat Ingredient Improves Jejunal and Hepatic Cholesterol Homeostasis in a Late-Stage Type 2 Diabetes Mellitus Rat Model, *Foods*, 2024, **13**, 1794.

29 M. Hernández-Martín, A. Macho-González, A. Garcimartín, M. E. López-Oliva, A. Bocanegra, R. Redondo-Castillejo, S. Bastida, J. Benedí and F. J. Sánchez-Muniz, Silicon-enriched meat positively improves plasma lipidaemia and lipoproteinaemia, LDLr, and insulin capability and the signalling pathway induced by an atherogenic diet in late-stage type 2 diabetes mellitus rats, *Food Funct.*, 2024, **15**, 1513–1526.

30 A. Macho-González, M. E. López-Oliva, J. J. Merino, R. A. García-Fernández, A. Garcimartín, R. Redondo-Castillejo, S. Bastida, F. J. Sánchez-Muniz and J. Benedí, Carob fruit extract-enriched meat improves pancreatic beta-cell dysfunction, hepatic insulin signaling and lipogenesis in late-stage type 2 diabetes mellitus model, *J. Nutr. Biochem.*, 2020, **84**, 108461.

31 A. Garcimartín, J. A. Santos-López, J. Benedí, S. Bastida and F. J. Sánchez-Muniz, Effects of silicon inclusion in restructured meat-enriched diet on lipoprotein profile and composition in aged wistar rats, *Atherosclerosis*, 2014, **235**, e202–e203.

32 AOAC International, Official Method 925.10: Moisture in Flour, in *Official Methods of Analysis 17th edition*, AOAC Publications, 2001.

33 R. O. David, F. J. Sánchez-Muniz, S. Bastida, J. Benedi and M. J. González-Muñoz, Gastric emptying and short-term digestibility of thermally oxidized sunflower oil used for

frying in fasted and nonfasted rats, *J. Agric. Food Chem.*, 2010, **58**, 9242–9248.

34 L. Apaza-Ticona, B. Pérez-Uz, M. T. García-Esteban, F. Aguilar-Rico and K. Slowing, Anti-melanogenic and Anti-inflammatory Activities of Hibiscus sabdariffa, *Rev. Bras. Farmacogn.*, 2022, **32**, 127–132.

35 I. Durak, Z. Yurtarslanl, O. Canbolat and Ö. Akyol, A methodological approach to superoxide dismutase (SOD) activity assay based on inhibition of nitroblue tetrazolium (NBT) reduction, *Clin. Chim. Acta*, 1993, **214**, 103–104.

36 H. Aebi, Catalase in vitro, *Methods Enzymol.*, 1984, **105**, 121–126.

37 I. Carlberg and B. Mannervik, Glutathione reductase, *Methods Enzymol.*, 1985, **113**, 484–490.

38 L. Flohé and W. A. Günzler, Assays of glutathione peroxidase, *Methods Enzymol.*, 1984, **105**, 114–120.

39 M. M. Bradford, A rapid and sensitive method for the quantitation of microgram quantities of protein utilizing the principle of protein-dye binding, *Anal. Biochem.*, 1976, **72**, 248–254.

40 B. Ou, M. Hampsch-Woodill and R. L. Prior, Development and validation of an improved oxygen radical absorbance capacity assay using fluorescein as the fluorescent probe, *J. Agric. Food Chem.*, 2001, **49**, 4619–4626.

41 A. P. Senft, T. P. Dalton and H. G. Shertzer, Determining glutathione and glutathione disulfide using the fluorescence probe o-phthalaldehyde, *Anal. Biochem.*, 2000, **280**, 80–86.

42 A. Macho-González, A. Garcimartín, N. Redondo, S. Cofrades, S. Bastida, E. Nova, J. Benedí, F. J. Sánchez-Muniz, A. Marcos and M. Elvira López-Oliva, Carob fruit extract-enriched meat, as preventive and curative treatments, improves gut microbiota and colonic barrier integrity in a late-stage T2DM model, *Food Res. Int.*, 2021, **141**, 110124.

43 D. Álvarez-Cilleros, S. Ramos, M. E. López-Oliva, F. Escrivá, C. Álvarez, E. Fernández-Millán and M.Á Martín, Cocoa diet modulates gut microbiota composition and improves intestinal health in Zucker diabetic rats, *Food Res. Int.*, 2020, **132**, 109058.

44 M. Hernández-Martín, A. Garcimartín, A. Bocanegra, A. Macho-González, R. A. García-Fernández, S. de Pascual-Teresa, R. Redondo-Castillejo, S. Bastida, F. J. Sánchez-Muniz, J. Benedí and M. E. López-Oliva, Silicon-Enriched Meat Ameliorates Diabetic Dyslipidemia by Improving Cholesterol, Bile Acid Metabolism and Ileal Barrier Integrity in Rats with Late-Stage Type 2 Diabetes, *Int. J. Mol. Sci.*, 2024, **25**, 11405.

45 A. Jusakul, P. Yongvanit, W. Loilome, N. Namwat and R. Kuver, Mechanisms of oxysterol-induced carcinogenesis, *Lipids Health Dis.*, 2011, **10**, 1–8.

46 B. Hippe, M. Remely, E. Aumueller, A. Pointner, U. Magnet and A. G. Haslberger, Faecalibacterium prausnitzii phylotypes in type two diabetic, obese, and lean control subjects, *Benefic. Microbes*, 2016, **7**, 511–517.

47 T. U. Maioli, E. Borras-Nogues, L. Torres, S. C. Barbosa, V. D. Martins, P. Langella, V. A. Azevedo and J. M. Chatel, Possible Benefits of Faecalibacterium prausnitzii for Obesity-Associated Gut Disorders, *Front. Pharmacol.*, 2021, **12**, 740636.

48 H. Liang, F. Jiang, R. Cheng, Y. Luo, J. Wang, Z. Luo, M. Li, X. Shen and F. He, A high-fat diet and high-fat and high-cholesterol diet may affect glucose and lipid metabolism differentially through gut microbiota in mice, *Exp. Anim.*, 2021, **70**, 73–83.

49 Y. Sugawara, A. Kanazawa, M. Aida, Y. Yoshida, Y. Yamashiro and H. Watada, Association of gut microbiota and inflammatory markers in obese patients with type 2 diabetes mellitus: post hoc analysis of a synbiotic interventional study, *Biosci. Microbiota, Food Health*, 2022, **41**, 103–111.

50 P. D. Cani, M. Osto, L. Geurts and A. Everard, Involvement of gut microbiota in the development of low-grade inflammation and type 2 diabetes associated with obesity, *Gut Microbes*, 2012, **3**(4), 279–288.

51 C. Chelakkot, J. Ghim and S. H. Ryu, Mechanisms regulating intestinal barrier integrity and its pathological implications, *Exp. Mol. Med.*, 2018, **50**(8), 1–9.

52 T. Arora and V. Tremaroli, Therapeutic Potential of Butyrate for Treatment of Type 2 Diabetes, *Front. Endocrinol.*, 2021, **12**, 761834.

53 K. H. Allin, V. Tremaroli, R. Caesar, B. A. H. Jensen, M. T. F. Damgaard, M. I. Bahl, T. R. Licht, T. H. Hansen, T. Nielsen, T. M. Dantoft, A. Linneberg, T. Jørgensen, H. Vestergaard, K. Kristiansen, P. W. Franks, T. Hansen, F. Bäckhed and O. Pedersen, Aberrant intestinal microbiota in individuals with prediabetes, *Diabetologia*, 2018, **61**, 810–820.

54 E. F. Stange and B. O. Schroeder, Microbiota and mucosal defense in IBD: an update, *Expert Rev. Gastroenterol. Hepatol.*, 2019, **13**, 963–976.

55 S. Fujisaka, Y. Watanabe and K. Tobe, The gut microbiome: a core regulator of metabolism, *J. Endocrinol.*, 2023, **256**(3), e220111.

56 T. P. M. Scheithauer, E. Rampanelli, M. Nieuwdorp, B. A. Vallance, C. B. Verchere, D. H. van Raalte and H. Herrema, Gut Microbiota as a Trigger for Metabolic Inflammation in Obesity and Type 2 Diabetes, *Front. Immunol.*, 2020, **11**, 571731.

57 C. Song, Z. Chai, S. Chen, H. Zhang, X. Zhang and Y. Zhou, Intestinal mucus components and secretion mechanisms: what we do and do not know, *Exp. Mol. Med.*, 2023, **55**(4), 681–691.

58 F. Suriano, E. E. L. Nyström, D. Sergi and J. K. Gustafsson, Diet, microbiota, and the mucus layer: The guardians of our health, *Front. Immunol.*, 2022, **13**, 953196.

59 F. Vernia, S. Longo, G. Stefanelli, A. Viscido and G. Latella, Dietary Factors Modulating Colorectal Carcinogenesis, *Nutrients*, 2021, **13**, 1–13.

60 L. Kruidenier and H. W. Verspaget, Review article: oxidative stress as a pathogenic factor in inflammatory bowel disease–radicals or ridiculous?, *Aliment. Pharmacol. Ther.*, 2002, **16**, 1997–2015.

61 G. Leonarduzzi, P. Gamba, B. Sottero, A. Kadl, F. Robbesyn, R. A. Calogero, F. Biasi, E. Chiarpotto, N. Leitinger, A. Sevanian and G. Poli, Oxysterol-induced up-regulation of

MCP-1 expression and synthesis in macrophage cells, *Free Radicals Biol. Med.*, 2005, **39**, 1152–1161.
62 M. Y. Zeng, N. Inohara and G. Nuñez, Mechanisms of inflammation-driven bacterial dysbiosis in the gut, *Mucosal Immunol.*, 2017, **10**, 18–26.
63 D. N. Jackson and A. L. Theiss, Gut bacteria signaling to mitochondria in intestinal inflammation and cancer, *Gut Microbes*, 2020, **11**, 285–304.
64 P. D. Cani, R. Bibiloni, C. Knauf, A. Waget, A. M. Neyrinck, N. M. Delzenne and R. Burcelin, Changes in gut microbiota control metabolic endotoxemia-induced inflammation in high-fat diet-induced obesity and diabetes in mice, *Diabetes*, 2008, **57**, 1470–1481.
65 P. D. Cani, J. Amar, M. A. Iglesias, M. Poggi, C. Knauf, D. Bastelica, A. M. Neyrinck, F. Fava, K. M. Tuohy, C. Chabo, A. Waget, E. Delmée, B. Cousin, T. Sulpice, B. Chamontin, J. Ferrières, J. F. Tanti, G. R. Gibson, L. Casteilla, N. M. Delzenne, M. C. Alessi and R. Burcelin, Metabolic endotoxemia initiates obesity and insulin resistance, *Diabetes*, 2007, **56**, 1761–1772.
66 V. W. M. Virginio, V. S. Nunes, F. A. Moura, F. H. Menezes, N. A. Andreollo, F. Rogerio, D. Z. Scherrer, E. C. R. Quintão, E. Nakandakare, O. Petrucci, W. Nadruz, E. C. De Faria and A. C. Sposito, Arterial tissue and plasma concentration of enzymatic-driven oxysterols are associated with severe peripheral atherosclerotic disease and systemic inflammatory activity, *Free Radical Res.*, 2015, **49**, 199–203.
67 A. J. Brown and W. Jessup, Oxysterols and atherosclerosis, *Atherosclerosis*, 1999, **142**, 1–28.
68 M. Y. Sun, A. J. Linsenbardt, C. M. Emnett, L. N. Eisenman, Y. Izumi, C. F. Zorumski and S. Mennerick, 24(S)-Hydroxycholesterol as a modulator of neuronal signaling and survival, *Neuroscientist*, 2016, **22**, 132.
69 D. K. Mandaliya and S. Seshadri, Short Chain Fatty Acids, pancreatic dysfunction and type 2 diabetes, *Pancreatology*, 2019, **19**, 280–284.
70 R. Redondo-Castillejo, A. Garcimartín, M. Hernández-Martín, M. E. López-Oliva, A. Bocanegra, A. Macho-González, S. Bastida, J. Benedí and F. J. Sánchez-Muniz, Proanthocyanidins: Impact on Gut Microbiota and Intestinal Action Mechanisms in the Prevention and Treatment of Metabolic Syndrome, *Int. J. Mol. Sci.*, 2023, **24**(6), 5369.
71 J. Plat, J. A. Nichols and R. P. Mensink, Plant sterols and stanols: effects on mixed micellar composition and LXR (target gene) activation, *J. Lipid Res.*, 2005, **46**, 2468–2476.
72 R. Jugdaohsingh, A. I. E. Watson, L. D. Pedro and J. J. Powell, The decrease in silicon concentration of the connective tissues with age in rats is a marker of connective tissue turnover, *Bone*, 2015, **75**, 40–48.
73 J. A. Grondin, Y. H. Kwon, P. M. Far, S. Haq and W. I. Khan, Mucins in Intestinal Mucosal Defense and Inflammation: Learning From Clinical and Experimental Studies, *Front. Immunol.*, 2020, **11**, 2054.
74 K. A. Kuhn, I. Pedraza and M. K. Demoruelle, Mucosal immune responses to microbiota in the development of autoimmune disease, *Rheum. Dis. Clin. North Am.*, 2014, **40**, 711–725.
75 A. P. Corfield, Mucins: A biologically relevant glycan barrier in mucosal protection, *Biochim. Biophys. Acta, Gen. Subj.*, 2015, **1850**, 236–252.
76 Y. Zhang, X. Zhu, X. Yu, P. Novák, Q. Gui and K. Yin, Enhancing intestinal barrier efficiency: A novel metabolic diseases therapy, *Front. Nutr.*, 2023, **10**, 1120168.
77 W. T. Kuo, M. A. Odenwald, J. R. Turner and L. Zuo, Tight junction proteins occludin and ZO-1 as regulators of epithelial proliferation and survival, *Ann. N. Y. Acad. Sci.*, 2022, **1514**, 21–33.
78 E. J. Kim, S. Y. Bu, M. K. Sung, M. H. Kang and M. K. Choi, Analysis of antioxidant and anti-inflammatory activity of silicon in murine macrophages, *Biol. Trace Elem. Res.*, 2013, **156**, 329–337.
79 J. A. David, W. J. Rifkin, P. S. Rabbani and D. J. Ceradini, The Nrf2/Keap1/ARE Pathway and Oxidative Stress as a Therapeutic Target in Type II Diabetes Mellitus, *J. Diabetes Res.*, 2017, 4826724.
80 R. Singh, S. Chandrashekharappa, S. R. Bodduluri, B. V. Baby, B. Hegde, N. G. Kotla, A. A. Hiwale, T. Saiyed, P. Patel, M. Vijay-Kumar, M. G. I. Langille, G. M. Douglas, X. Cheng, E. C. Rouchka, S. J. Waigel, G. W. Dryden, H. Alatassi, H. G. Zhang, B. Haribabu, P. K. Vemula and V. R. Jala, Enhancement of the gut barrier integrity by a microbial metabolite through the Nrf2 pathway, *Nat. Commun.*, 2019, **10**, 1–18.
81 P. Du, X. Zhang, K. Luo, Y. Li, C. Fu, J. Xiao and Q. Xiao, Curculigoside mitigates hepatic ischemia/reperfusion-induced oxidative stress, inflammation, and apoptosis via activation of the Nrf-2/HO-1 pathway, *Hum. Exp. Toxicol.*, 2022, **41**, 9603271221087146.
82 K. M. Holmström and T. Finkel, Cellular mechanisms and physiological consequences of redox-dependent signalling, *Nat. Rev. Mol. Cell Biol.*, 2014, **15**, 411–421.
83 C. Kunst, S. Schmid, M. Michalski, D. Tümen, J. Buttenschön, M. Müller and K. Gülow, The Influence of Gut Microbiota on Oxidative Stress and the Immune System, *Biomedicines*, 2023, **11**, 1388.
84 W. Y. Wu, P. L. Chou, J. C. Yang and C. T. Chien, Silicon-containing water intake confers antioxidant effect, gastrointestinal protection, and gut microbiota modulation in the rodents, *PLoS One*, 2021, **16**(3), e0248508.
85 P. Palozza, R. Simone, A. Catalano, G. Monego, A. Barini, M. C. Mele, N. Parrone, S. Trombino, N. Picci and F. O. Ranelletti, Lycopene prevention of oxysterol-induced proinflammatory cytokine cascade in human macrophages: inhibition of NF-κB nuclear binding and increase in PPARγ expression, *J. Nutr. Biochem.*, 2011, **22**, 259–268.
86 D. I. Jang, A. H. Lee, H. Y. Shin, H. R. Song, J. H. Park, T. B. Kang, S. R. Lee and S. H. Yang, The Role of Tumor Necrosis Factor Alpha (TNF-α) in Autoimmune Disease and Current TNF-α Inhibitors in Therapeutics, *Int. J. Mol. Sci.*, 2021, **22**, 1–16.
87 R. M. Jones and A. S. Neish, Redox Signaling Mediated by the Gut Microbiota, *Free Radical Res.*, 2013, **47**, 950.